Integer and fractional quantum hall effects in lattice magnets

Venderbos, J.W.F.

Appendices

APPENDIX A

DETAILS OF LATTICES

In the present Appendix we collect all details and relevant definitions pertaining to the four lattices that have been treated in the main text. These include explicit expressions for lattice vectors, reciprocal lattice vectors, special ordering momenta, and the Hamiltonians for lattice fermions hopping on the respective lattices. We first give the details of the square lattice and then present details of the hexagonal lattices. In case of the triangular and honeycomb lattices we include expressions for the mean field orbital momentum basis functions. For both the honeycomb and kagome lattices we also provide a more detailed derivation of the lattice symmetries of Dirac matrices, the results of which are used in the main text. In case of the kagome lattice we provide more details on explicit expressions for density wave states discussed in main text.

Before we come to the individual lattices, let us list a number of general definitions applicable to all lattives in order to avoid repetition. In Section 9.1.1 the lattice basis vectors were defined as $\vec{x}_1$ and $\vec{x}_2$. In expressions for Hamiltonians in momentum space it is convenient to abbreviate the inner products $\vec{k} \cdot \vec{x}_i$ as k_i and we will consistently do so. In addition, we write T_i for the exponentials $T_i \equiv e^{i\vec{k}\cdot\vec{x}_i}$.

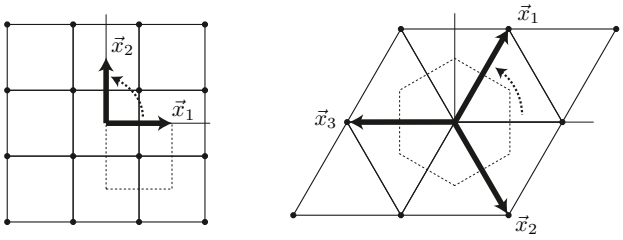

Figure A.1: Schematic picture of two of the four lattices considered in this work. (left) the square lattice, (right) triangular lattice. Lattice basis vectors are represented as thick back arrows, the hexagonal lattices also show $\vec{x}_3 = -\vec{x}_1 - \vec{x}_2$. The curved dashed arrows indicate the fourfold (C_4) and sixfold (C_6) rotations of the square and hexagonal lattices, respectively.

A.1 Square lattice

The square Bravais lattice is defined in terms of the lattice basis vectors

$$\vec{x}_1 = a \begin{bmatrix} 1 \\ 0 \end{bmatrix}, \qquad \vec{x}_2 = a \begin{bmatrix} 0 \\ 1 \end{bmatrix}, \tag{A.1}$$

which generate the translations $T(\vec{x}_1)$ and $T(\vec{x}_2)$. Here a is the lattice constant, i.e. the distance between two nearest neighbors of the square lattice. The reciprocal lattice is a square lattice in momentum space generated by the vectors

$$\vec{G}_1 = \frac{2\pi}{a} \begin{bmatrix} 1 \\ 0 \end{bmatrix}, \qquad \vec{G}_2 = \frac{2\pi}{a} \begin{bmatrix} 0 \\ 1 \end{bmatrix}, \tag{A.2}$$

A schematic picture of both the real space lattice and the reciprocal lattice is presented in Figs. A.1 and A.3. As is shown in Fig. A.1, in this work we choose to place the origin at the center of a square. We found this to be the most convenient choice, in addition to being consistent with the (obvious) choices made for the hexagonal lattices (see below). This choice does however have the consequence that the atomic positions are displaced from the Bravais lattice vectors by an amount

$$\vec{l} = \frac{a}{2} \begin{bmatrix} 1 \\ -1 \end{bmatrix}. \tag{A.3}$$

Contrary to the convention of equating the atomic positions and Bravais lattice vectors, the present choice implies that point group operations must be associated with a

nontrivial lattice translation $\vec{t}$ when acting on an atomic position. For example, referring to Section 9.1.1, we have $C_4\vec{l} = \vec{x}_2 + \vec{l}$ where $\vec{t} = \vec{x}_2$. This minor complication notwithstanding, it is the most convenient and consistent convention.

The square lattice Hamiltonian $\hat{H}$ and corresponding electronic dispersion are simply given by

$$\hat{H} = \sum_{\vec{k}} E(\vec{k})\hat{\psi}^\dagger(\vec{k})\hat{\psi}(\vec{k}), \quad E(\vec{k}) = -2t\sum_{i=1}^{2}\cos k_i. \tag{A.4}$$

A.2 Triangular lattice

The triangular Bravais lattice is generated by the two lattice basis vectors

$$\vec{x}_1 = \frac{a}{2}\begin{bmatrix}1\\ \sqrt{3}\end{bmatrix}, \quad \vec{x}_2 = \frac{a}{2}\begin{bmatrix}1\\ -\sqrt{3}\end{bmatrix}, \tag{A.5}$$

and in addition to these we define for convenience the (linearly dependendent) lattice vector $\vec{x}_3 = -\vec{x}_1 - \vec{x}_2$. Again, a is the lattice constant. In case of the triangular lattice we choose the origin to at one of the Bravais lattice points, as indicated in Fig. A.1 on the upper right.

The reciprocal lattice of a triangular lattice is a triangular lattice and the reciprocal lattice vectors are given by

$$\vec{G}_1 = \frac{2\pi}{a}\begin{bmatrix}1\\ 1/\sqrt{3}\end{bmatrix}, \qquad \vec{G}_2 = \frac{2\pi}{a}\begin{bmatrix}1\\ -1/\sqrt{3}\end{bmatrix}. \tag{A.6}$$

The corresponding first Brillouin zone is graphically shown in Fig. A.3. The M-point ordering momenta $\vec{Q}_\mu$ are shown in Fig. A.3 by full red dots and their explicit expressions are

$$\vec{Q}_{1,3} = \frac{\pi}{a\sqrt{3}}\begin{bmatrix}\pm\sqrt{3}\\ 1\end{bmatrix}, \quad \vec{Q}_2 = \frac{2\pi}{a\sqrt{3}}\begin{bmatrix}0\\ 1\end{bmatrix}. \tag{A.7}$$

The triangular lattice Hamiltonian $\hat{H}$ and corresponding electronic dispersion are simply given by

$$\hat{H} = \sum_{\vec{k}} E(\vec{k})\hat{\psi}^\dagger(\vec{k})\hat{\psi}(\vec{k}), \quad E(\vec{k}) = -2t\sum_{i=1}^{3}\cos k_i. \tag{A.8}$$

A.2.1 Mean field orbital momentum basis functions

In Section 9.2.3 we have discussed how to set up a triangular lattice spinful mean-field theory anticipating translational symmetry breaking due to finite $\vec{Q}_\mu$ ordering vectors. The nearest neighbor interaction V_{ij} required a decomposition into the orbital momentum functions transforming as irreducible representations of the hexagonal point group. Here we list these functions explicitly.

In general the orbital momentum functions $\lambda^{(n,\mathcal{I}_r)}(\vec{k})$ are labeled by n (n-th nearest neighbor) and $\mathcal{I}_r$ (irreducible representation $\mathcal{I}$ and partner r). In case of the triangular lattice we have only considered $n = 1$ and found that we need to sum over four irreducible representations, two of them $1D$ and two of them $2D$. The $1D$ representation A_1 and the $2D$ representation E_2 functions are constructed from cosine functions and take the form

$$\begin{aligned} \lambda^{(1,A_1)}(\vec{k}) &= \frac{1}{\sqrt{3}}(\cos k_1 + \cos k_2 + \cos k_3) \\ \vec{\lambda}^{(1,E_2)}(\vec{k}) &= \frac{1}{\sqrt{2}}\begin{bmatrix} \frac{1}{\sqrt{3}}(-2\cos k_1 + \cos k_2 + \cos k_3) \\ \cos k_2 - \cos k_3 \end{bmatrix}. \end{aligned} \tag{A.9}$$

Instead, the $1D$ representation B_1 and the $2D$ representation E_1 functions are constructed from sine functions and read

$$\begin{aligned} \lambda^{(1,B_1)}(\vec{k}) &= \frac{1}{\sqrt{3}}(\sin k_1 + \sin k_2 + \sin k_3) \\ \vec{\lambda}^{(1,E_1)}(\vec{k}) &= \frac{1}{\sqrt{2}}\begin{bmatrix} \frac{1}{\sqrt{3}}(-2\sin k_1 + \sin k_2 + \sin k_3) \\ \sin k_2 - \sin k_3 \end{bmatrix}. \end{aligned} \tag{A.10}$$

The triangular lattice function $\Gamma^{(1)}(\vec{k} - \vec{k}')$ can therefore be expanded in separable functions $\lambda^{(1,\mathcal{I}_r)}(\vec{k})$ and $\lambda^{(1,\mathcal{I}_r)}(\vec{k}')$ as

$$\Gamma^{(1)}(\vec{k} - \vec{k}') = \sum_{\mathcal{I},r} \lambda^{(1,\mathcal{I}_r)}(\vec{k})\lambda^{(1,\mathcal{I}_r)}(\vec{k}') \tag{A.11}$$

with $\mathcal{I} = A_1, E_2, B_1, E_1$. Since all functions are real we have suppressed the complex conjugation operation.

A.3 Honeycomb lattice

The Bravais lattice of the honeycomb lattice is a triangular lattice and the honeycomb lattice unit cell contains two inequivalent atoms, which are labeled as the A and B

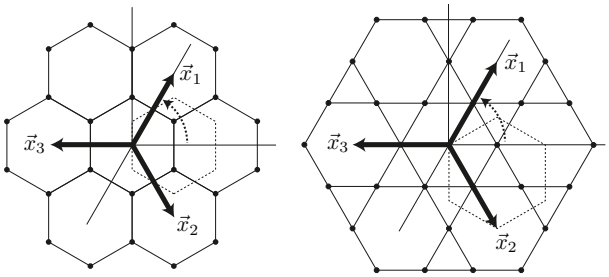

Figure A.2: Schematic picture of two of the four lattices considered in this work. (left) the honeycomb lattice, (right) kagome lattice. Lattice basis vectors are represented as thick back arrows, the hexagonal lattices also show $\vec{x}_3 = -\vec{x}_1 - \vec{x}_2$. The curved dashed arrows indicate the sixfold (C_6) rotations of the hexagonal lattices.

sublattices. The unit vectors of the triangular Bravais lattice are taken to be the same as in Eq. (A.5),

$$\vec{x}_1 = \frac{a}{2}\begin{bmatrix} 1 \\ \sqrt{3} \end{bmatrix}, \qquad \vec{x}_2 = \frac{a}{2}\begin{bmatrix} 1 \\ -\sqrt{3} \end{bmatrix}, \tag{A.12}$$

where a is again the lattice consant, which in case of the honeycomb lattice is not the distance between nearest neighbors (i.e. the carbon-carbon distance in graphene). As was the case for the triangular lattice, we define $\vec{x}_3 \equiv -\vec{x}_1 - \vec{x}_2$. The origin is taken to be the center of a hexagon and two vectors $\vec{l}_A$ and $\vec{l}_B$, specifying the positions of the A and B atoms in the unit cell with respect to the origin, are given by

$$\vec{l}_A = \frac{a}{2}\begin{bmatrix} 1 \\ -1/\sqrt{3} \end{bmatrix}, \qquad \vec{l}_B = \frac{a}{2}\begin{bmatrix} 1 \\ 1/\sqrt{3} \end{bmatrix}. \tag{A.13}$$

Taking the A sublattice as a reference sublattice, we define the three nearest neighbor vectors connecting the sublattices as

$$\vec{\delta}_1 = \vec{l}_B - \vec{l}_A, \quad \vec{\delta}_2 = \vec{\delta}_1 - \vec{x}_1, \quad \vec{\delta}_3 = \vec{\delta}_1 + \vec{x}_2. \tag{A.14}$$

The reciprocal lattice of a triangular lattice is a triangular lattice, as was noted previously, and in the case of the honeycomb lattice the reciprocal lattice vectors coincide with those of the triangular lattice,

$$\vec{G}_1 = \frac{2\pi}{a}\begin{bmatrix} 1 \\ 1/\sqrt{3} \end{bmatrix}, \qquad \vec{G}_2 = \frac{2\pi}{a}\begin{bmatrix} 1 \\ -1/\sqrt{3} \end{bmatrix}. \tag{A.15}$$

The electronic honeycomb lattice Hamiltonian is given by

$$\hat{H} = \sum_{\vec{k}} \hat{\psi}_i^\dagger(\vec{k}) \mathcal{H}_{ij}(\vec{k}) \hat{\psi}_j(\vec{k}), \tag{A.16}$$

where i, j label the sublattices and the $\vec{k}$-dependent matrix takes the form

$$\mathcal{H}(\vec{k}) = -t \begin{bmatrix} 0 & 1 + T_2 + T_1^* \\ 1 + T_2^* + T_1 & 0 \end{bmatrix} \tag{A.17}$$

with the T_i as defined at the beginning of this appendix. It is a very well-known fact that the honeycomb band structure displays band touchings at the Brioullin zone vertices $\vec{K}_\pm$ which are given by

$$\vec{K}_\pm = \frac{4\pi}{3} \begin{bmatrix} \pm 1 \\ 0 \end{bmatrix}. \tag{A.18}$$

At these isolated band touchings, which are protected by lattice symmetries (c.f. section A.3.1), the electronic bands disperse linearly, and the nodes are therefore referred to as Dirac points, or K-points. These Dirac points are shown in Fig. A.3 on the left side by large blue dots. In the main text we have discussed K-point ordering on the honeycomb lattice.

The M-point ordering momenta are the same as for the triangular lattice (and shown in Fig. A.3) and we quote them here again for completeness

$$\vec{Q}_{1,3} = \frac{\pi}{a\sqrt{3}} \begin{bmatrix} \pm\sqrt{3} \\ 1 \end{bmatrix}, \quad \vec{Q}_2 = \frac{2\pi}{a\sqrt{3}} \begin{bmatrix} 0 \\ 1 \end{bmatrix}. \tag{A.19}$$

A.3.1 Point group protection of honeycomb Dirac points

In the Brillouin zone of the honeycomb lattice (one may think of graphene), or any other lattice with point group C_{6v} such as triangular and kagome, there are special $\vec{k}$ points that are left invariant under certain point group operations. Of particular, even profound, interest are the corners of the Brillouin zone hexagon given by $\vec{K}_\pm$ (see previous subsection), also called K-points or valleys. The terminology valley is inspired by the fact that at these points $\mathcal{H}(\vec{K}_\pm) = 0$, leading to a degeneracy in the spectrum. The little cogroup of each $\vec{K}_\pm$ is C_{3v} and consists of the threefold rotations $C_3 = C_6^2$ and $C_3^{-1} = C_6^4$ of the honeycomb lattice and the three reflection bisecting the bonds of the hexagon. These reflections exchange the A and B sublattice. The group C_{3v} admits a two dimensional irreducible representation, which is realized by

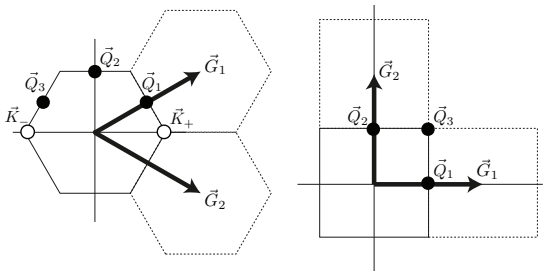

Figure A.3: Depiction of the Brillouin zones of the hexagonal lattices (left) and the square lattice (right). The reciprocal lattice vectors are denoted as $\vec{G}_1$ and $\vec{G}_2$. The special commensurate ordering momenta are indicated. For both the square and the hexagonal lattices there is a set $\vec{Q}_\mu$ (full dots), while in case of the hexagonal lattices there is a second set of two ordering vectors $\vec{K}_+$ and $\vec{K}_-$ (open dots).

the matrices $\mathcal{U}_R$ of equation (9.6) with $R \in C_{3v}$. Also note the remark following equation (9.10). In fact, by working out these matrices we derive the representation for $\vec{K}_+$ as

$$\mathcal{U}_I = \begin{bmatrix} 1 & 0 \\ 0 & 1 \end{bmatrix}, \quad \mathcal{U}_{C_3} = \begin{bmatrix} \omega & 0 \\ 0 & \omega^{-1} \end{bmatrix}, \quad \mathcal{U}_{C_3^{-1}} = \begin{bmatrix} \omega^{-1} & 0 \\ 0 & \omega \end{bmatrix},$$
$$\mathcal{U}_{\sigma_{v1}} = \begin{bmatrix} 0 & 1 \\ 1 & 0 \end{bmatrix}, \quad \mathcal{U}_{\sigma_{v2}} = \begin{bmatrix} 0 & \omega \\ \omega^{-1} & 0 \end{bmatrix}, \quad \mathcal{U}_{\sigma_{v3}} = \begin{bmatrix} 0 & \omega^{-1} \\ \omega & 0 \end{bmatrix}. \tag{A.20}$$

where we defined $\omega = e^{2\pi i/3}$. Strictly speaking, the representation for $\vec{K}_-$ is obtained by $\omega \leftrightarrow \omega^{-1}$. These matrices act on the Hamiltonian at the K-points, i.e. $\mathcal{H}(\vec{K}_\pm)$, which can be expanded in Pauli matrices τ^i. As $\vec{K}_\pm$ are invariant points under R we have $\mathcal{U}_R \mathcal{H}(\vec{K}_\pm)\mathcal{U}_R^\dagger = \mathcal{H}(\vec{K}_\pm)$, or $[\mathcal{U}_R, \mathcal{H}(\vec{K}_\pm)] = 0$. We may take $\mathcal{U}_{C_3}$ and $\mathcal{U}_{\sigma_{v1}}$ to show that this mandates $\mathcal{H}(\vec{K}_\pm) = I$ and the degeneracy is therefore protected exactly at $\vec{K}_\pm$ making it an essential degeneracy. To demontrate the vanishing of the commutator we just have to observe that $\mathcal{U}_{\sigma_{v1}} = \tau^1$ and $\mathcal{U}_{C_3}$ contains τ^3. The only matrix commuting with both is the unit matrix.

A.3.2 Symmetry of Dirac matrices

In this part we provide more details on the low-energy theory of the honeycomb lattice at half filling, which is described by a $2D$ Dirac Lagrangian. For an extensive discussion on the connection to $2+1D$ QED see [206]. Here we will be concerned

with symmetries of the dicrete point groups C_{6v} and C''_{6v} and more specifically the symmetry properties of low-energy spinor bilinears.

The low-energy theory in the vicinity of the two inequivalent valleys $\vec{K}_\pm$ is obtained by expanding the dispersion around these valleys $\vec{K}_\pm$ in small momenta $\vec{q}$. One obtains the Dirac Hamiltonian

$$\mathcal{H}(\vec{q}) = \hbar v_F (q_x \nu^3 \tau^1 + q_y \tau^2) \tag{A.21}$$

(where $v_F = \sqrt{3}ta/(2\hbar)$) acting on the spinor $\Phi(\vec{q})$ which is given by

$$\hat{\Phi}(\vec{q}) = \begin{bmatrix} \hat{\psi}_A(\vec{K}_+ + \vec{q}) \\ \hat{\psi}_B(\vec{K}_+ + \vec{q}) \\ \hat{\psi}_A(\vec{K}_- + \vec{q}) \\ \hat{\psi}_B(\vec{K}_- + \vec{q}) \end{bmatrix}. \tag{A.22}$$

The set of Pauli matrices ν^i acts on the valley degree of freedom and the τ^i matrices on the sublattice degre of freedom. Exchanging A and B sublattice for the $\vec{K}_-$ by a unitary transformation we obtain the chiral representation of the low-energy Hamiltonian

$$\mathcal{H}(\vec{q}) = \hbar v_F \nu^3 \vec{q} \cdot \vec{\tau}. \tag{A.23}$$

This chiral basis is the basis in which we will state the results. As the Dirac points have been folded to Γ the effect of the generators of the space is found by making use of equation (9.18). The generators may be used directly to generate all operations in the space group. Note that

$$\hat{\Phi} \equiv \hat{\Phi}(\vec{0}) = \begin{bmatrix} \hat{\chi}_{A1}(\vec{0}) \\ \hat{\chi}_{B1}(\vec{0}) \\ \hat{\chi}_{A2}(\vec{0}) \\ \hat{\chi}_{B2}(\vec{0}) \end{bmatrix}. \tag{A.24}$$

With this it is straightforward to dedude that the translation operator $T(\vec{x}_1)$ acts as

$$T(\vec{x}_1) \quad \rightarrow \quad \begin{bmatrix} \omega & & & \\ & \omega & & \\ & & \omega^{-1} & \\ & & & \omega^{-1} \end{bmatrix} \hat{\Phi}, \tag{A.25}$$

(again $\omega = e^{2\pi i/3}$) while the six-fold rotation C_6 acts as

$$C_6 \quad \rightarrow \quad \begin{bmatrix} & & & 1 \\ & & \omega & \\ & 1 & & \\ \omega^{-1} & & & \end{bmatrix} \hat{\Phi}, \tag{A.26}$$

note that this is diagonal in valley space as the six-fold rotation exchanges $\vec{K}_\pm$. The reflection σ_v acts as

$$\sigma_v \quad \rightarrow \quad \tau^1 \hat{\Phi}. \tag{A.27}$$

In addition to the space group generators it will be convenient to classify low-energy bilinears based on their transformation property under time-reversal. Hence, time-reversal is found to be represented by

$$\mathcal{T} \quad \rightarrow \quad \mathcal{K}\nu^1 \hat{\Phi}, \tag{A.28}$$

where $\mathcal{K}$ denotes complex conjugation. Note that this implies that $\nu^3\tau^1$ and τ^2 are both odd, as they should be. They are coupled linearly to $\vec{q}$, which is also odd.

The free Dirac Hamiltonian consists of the matrices $\nu^3\tau^1$ and τ^2. Spectral gaps are generated by Dirac matrices which anti-commute with these. It is a simple matter to find the four matrices which have this property, and they are found to be τ^3, $\nu^3\tau^3$, $\nu^1\tau^1$ and $\nu^2\tau^1$. Using the action of time-reversal one easily sees that while $\nu^3\tau^3$ is odd, the other three are even under time-reversal. The time-reversal invariant Dirac matrices all anti-commute between themselves and together with $\nu^3\tau^1$ and τ^2 they constitute the set of maximally anti-commuting Hermitian 4×4-matrices. Based on the action of the generators of the symmetry group, we can assign the masses to representations of C_{6v}''' and C_{6v}. Taking the time-reversal invariant masses first, we find that τ^3 transforms as B_2, while $\nu^1\tau^1$ and $\nu^2\tau^1$ are partners of the representation E_1'. The latter can be decomposed into $A_1 \oplus B_1$ and the following linear combinations are found to correspond to this decomposition

$$\begin{aligned} A_1 \;&\rightarrow\; \cos\theta\nu^1\tau^1 + \sin\theta\nu^2\tau^1 \\ B_1 \;&\rightarrow\; -\sin\theta\nu^1\tau^1 + \cos\theta\nu^2\tau^1, \end{aligned} \tag{A.29}$$

where $\theta = \pi/3$ The time-reversal breaking mass term $\nu^3\tau^3$ is found to transform as A_2. There are three Dirac matrices which lift the degeneracy between the valleys, but preserve the twofold degeneracy within each valley and since they distinguish the valleys at $\vec{K}_\pm$ which are related by time-reversal, all three are time-reversal symmetry breaking. The three matrices are ν^3, $\nu^1\tau^2$ and $\nu^2\tau^2$. The matrix ν^3 can be shown

Irreps of C_{6v}'' Irreps of C_{6v}	A_2	B_1	B_2	E_1	E_2
(standard)	$\nu^3\tau^3$	ν^3	τ^3	$\nu^3\tau^1$, τ^2	τ^1, $\nu^3\tau^2$
(chiral)	τ^3	ν^3	$\tau^3\tau^3$	$\nu^3\tau^1$, $\nu^3\tau^2$	τ^1, τ^2
	E_1'	E_2'		G'	
	$A_1 \oplus B_1$	$A_2 \oplus B_2$		$E_1 \oplus E_2$	
	$\nu^1\tau^1$, $\nu^2\tau^1$	$\nu^1\tau^2$, $\nu^2\tau^2$		ν^1 , ν^2, $\nu^1\tau^3$, $\nu^2\tau^3$	
	ν^1, ν^2	$\nu^1\tau^3$, $\nu^2\tau^3$		$\nu^1\tau^1$, $\nu^2\tau^1$, $\nu^1\tau^2$, $\nu^2\tau^2$	

Table A.1: This table summarizes the identification of low-energy fermion bilinears as basis functions of irreducible representations of C_{6v}'''. In addition we present the irreducible representations of C_{6v} contained in those of C_{6v}''.

to transform according to B_1, while $\nu^1\tau^2$ and $\nu^2\tau^2$ are partners of E_2'. They can be written as basis functions transforming as A_2 and B_2 in the following way

$$\begin{aligned} A_2 &\rightarrow \sin\theta\nu^1\tau^2 + \cos\theta\nu^2\tau^2 \\ B_2 &\rightarrow \cos\theta\nu^1\tau^2 - \sin\theta\nu^2\tau^2. \end{aligned} \tag{A.30}$$

Of the remaining six Dirac matrices, two are diagonal in valley space, while the other four exchange valleys. The former are τ^1 and $\nu^3\tau^2$, which are time-reversal invariant and are partners of E_2. Indeed, as they do not originate from a coupling of $\vec{K}_\pm$ they should correspond to the translationally invariant content of the symmetry classification. The set of matrices which do originate from coupling are ν^1, ν^2, $\nu^1\tau^3$ and $\nu^2\tau^3$, all of which are time-reversal invariant. Together they transform as G' of the group C_{6v}'''.

A.3.3 Lifting of degeneracies at M' points

We now present the details of degeneracy protection and lifting at the M' points of the reduced BZ corresponding to M-point order, i.e. order parameter components at $\vec{Q}_\mu$. It was mentioned in Section 9.4.1, if the translations $T(\vec{x}_i)$ and the M'-invariant elements C_{2v} are good symmetries then two-fold degeneracies at the M' points are protected, while in case of C_{2v} symmetry only, i.e. broken translations, there are no symmetry protected degeneracies. Here we demonstrate this explicitly. The recipy is

by now familiar and we write the state operator at $\vec{M}' = \vec{Q}_2/2$ as.

$$\hat{\Phi}_{\mathrm{M}'} = \begin{bmatrix} \hat{\psi}_j(\vec{M}') \\ \hat{\psi}_j(\vec{M}' + \vec{Q}_1) \\ \hat{\psi}_j(\vec{M}' + \vec{Q}_2) \\ \hat{\psi}_j(\vec{M}' + \vec{Q}_3) \end{bmatrix}. \tag{A.31}$$

The action of the translations $T(\vec{x}_1)$ and $T(\vec{x}_2)$ (up to global $U(1)$ phases) is easily derived to be

$$T(\vec{x}_1) \;\rightarrow\; \begin{bmatrix} 1 & & & \\ & -1 & & \\ & & -1 & \\ & & & 1 \end{bmatrix} \equiv \rho^3\nu^3 \tag{A.32}$$

where the matrix entries should be understood as 2×2 unit matrices (τ^0) and we have introduced another set of Pauli matrices ρ^i to generate the 8×8 representation. Then $T(\vec{x}_2)$ is given by ρ^3. For the C_2 element we derive

$$C_2 \;\rightarrow\; \begin{bmatrix} & & \tau^1 & \\ & & & -\tau^1 \\ \tau^1 & & & \\ & \tau^1 & & \end{bmatrix} \equiv \rho^1\nu^3\tau^1. \tag{A.33}$$

Symmetry dictates that the Hamiltonian at M' must commute with these elements. Taking just these translation and the inversion we simply see that the only allowed terms are $\nu^3\tau^1$ and ν^3. This observation already completes the task of proving that two-fold degeneracies must exist, since any linear combination of these two terms will be proportional to ρ^0. Hence, all eigenvalues of must appear twice. We check whether the two reflections σ_v and $C_2\sigma_v$ give any additional constraints. For σ_v we find

$$\sigma_v \;\rightarrow\; \begin{bmatrix} & & \tau^1 & \\ & \tau^1 & & \\ \tau^1 & & & \\ & & & \tau^1 \end{bmatrix} \equiv \rho^1\nu^3\tau^1, \tag{A.34}$$

and we may use the expression for C_2 to derive the action of the other reflection. We find no further symmetry constraints on the energy levels at M'.

Breaking the translations leads to the symmetry group C_{2v}, which does not have any $2D$ irreducible representation and therefore cannot protect degeneracies. Ignoring the constraints coming from the translation above, one observes that more terms are allowed on the Hamiltonian which in general will lift the degeneracies.

A.3.4 Mean-field momentum functions

In the same way as for the triangular lattice in Section A.2.1 we present the explicit orbital momentum fucntions which are used to decompose the nearest neighbor or next-nearest neighbor interactions. In Section 9.2.3 the basic structure of a mean field theory for both K-point and M-point order on the honeycomb lattice was discussed. Here we give explicit expressions for orbital momentum functions $\lambda_{ij}^{(n,\mathcal{I}_r)}(\vec{k})$ corresponding to $\Gamma_{ij}^{(1)}(\vec{k}-\vec{k}')$ and $\Gamma_{ij}^{(2)}(\vec{k}-\vec{k}')$.

The decomposition of the nearest neighbor interaction function $\Gamma_{ij}^{(1)}(\vec{k}-\vec{k}')$ consists of two irreducible representations. The first, A_1, is $1D$ and the second, E_2, $2D$. The orbital momentum functions are given by

$$\begin{aligned}
\lambda_{AB}^{(1,A_1)}(\vec{k}) &= \frac{1}{\sqrt{3}}(1+e^{-ik_1}+e^{ik_2}) \\
\vec{\lambda}_{AB}^{(1,E_2)}(\vec{k}) &= \frac{1}{\sqrt{2}}\begin{bmatrix} \frac{1}{\sqrt{3}}(-2+e^{-ik_1}+e^{ik_2}) \\ e^{-ik_1}-e^{ik_2} \end{bmatrix}.
\end{aligned} \tag{A.35}$$

Note that we would have $\lambda_{BA}^{(1,A_1)} = \lambda_{AB}^{(1,A_1)*}$ and the formula for the decomposition is given in Eq. (9.52).

The Bravais lattice of the honeycomb lattice is a triangular lattice and we can therefore directly infer the orbital momentum functions which decompose the next-nearest neighbor function $\Gamma_{ij}^{(2)}(\vec{k}-\vec{k}')$ from the triangular lattice case. Note that we can write $\lambda_{AA}^{(n,\mathcal{I}_r)} = \lambda_{BB}^{(n,\mathcal{I}_r)} = \lambda^{(n,\mathcal{I}_r)}$. The orbital momentum functions read explicitly

$$\begin{aligned}
\lambda^{(2,A_1)}(\vec{k}) &= \frac{1}{\sqrt{3}}(\cos k_1+\cos k_2+\cos k_3) \\
\vec{\lambda}^{(2,E_2)}(\vec{k}) &= \frac{1}{\sqrt{2}}\begin{bmatrix} \frac{1}{\sqrt{3}}(-2\cos k_1+\cos k_2+\cos k_3) \\ \cos k_2-\cos k_3 \end{bmatrix} \\
\lambda^{(2,B_1)}(\vec{k}) &= \frac{1}{\sqrt{3}}(\sin k_1+\sin k_2+\sin k_3) \\
\vec{\lambda}^{(2,E_1)}(\vec{k}) &= \frac{1}{\sqrt{2}}\begin{bmatrix} \frac{1}{\sqrt{3}}(-2\sin k_1+\sin k_2+\sin k_3) \\ \sin k_2-\sin k_3 \end{bmatrix},
\end{aligned} \tag{A.36}$$

i.e. there are the same four irreducible representations as in the triangular lattice nearest neighbor case.

A.4 Kagome lattice

The kagome lattice is another lattice with hexagonal symmetry, meaning that the Bravais lattice is triangular. However, the kagome lattice unit cell contains three inequivalent atoms, which are labeled by their sublattice index A, B and C. We choose the generators of lattice translations as

$$\vec{x}_1 = a\begin{bmatrix}1\\ \sqrt{3}\end{bmatrix}, \qquad \vec{x}_2 = a\begin{bmatrix}1\\ -\sqrt{3}\end{bmatrix}, \tag{A.37}$$

where a is taken as the length of a bond, i.e. the distance between nearest neighbors. In terms of a these vectors are half of the triangular and honeycomb lattice vectors. Hence, the reciprocal lattice vectors are twice as large as was the case for the triangular lattice, and are given by

$$\vec{G}_1 = \frac{\pi}{a}\begin{bmatrix}1\\ 1/\sqrt{3}\end{bmatrix}, \qquad \vec{G}_2 = \frac{\pi}{a}\begin{bmatrix}1\\ -1/\sqrt{3}\end{bmatrix}. \tag{A.38}$$

We take the origin to be the center of a hexagon of the kagome lattice and three vectors $\vec{l}_A$, $\vec{l}_B$ and $\vec{l}_C$ specifying the positions of the atoms in the unit cell with respect to the origin are given by

$$\vec{l}_A = \frac{a}{2}\begin{bmatrix}1\\ -\sqrt{3}\end{bmatrix}, \qquad \vec{l}_B = \frac{a}{2}\begin{bmatrix}3\\ -\sqrt{3}\end{bmatrix}, \qquad \vec{l}_C = a\begin{bmatrix}1\\ 0\end{bmatrix}. \tag{A.39}$$

Taking the A sublattice as a reference sublattice, we define the three nearest neighbor vectors connecting the sublattices as

$$\vec{\delta}_1 = \vec{l}_B - \vec{l}_A, \qquad \vec{\delta}_2 = \vec{l}_C - \vec{l}_B, \qquad \vec{\delta}_3 = \vec{l}_A - \vec{l}_C. \tag{A.40}$$

In addition to these vectors we also define the vectors connecting next-nearest neighbors on the kagome lattice. They are given by

$$\vec{\delta}'_1 = \vec{l}_C - 2\vec{l}_A, \qquad \vec{\delta}'_2 = -2\vec{l}_C + \vec{l}_A, \qquad \vec{\delta}'_3 = \vec{l}_A + 2\vec{l}_C. \tag{A.41}$$

The momentum dependent Hamiltonian of electrons hopping between nearest neighbors on the kagome lattice then takes the form

$$\mathcal{H}(\vec{k}) = -t\begin{bmatrix}0 & 1+T_1^*T_2^* & 1+T_1^*\\ 1+T_1T_2 & 0 & 1+T_2\\ 1+T_1 & 1+T_2^* & 0\end{bmatrix} \tag{A.42}$$

with the familiar definition of T_i. It is not uncommon in the context of the kagome lattice to take into account hopping between next-nearest neighbors in the tight-binding

Hamiltonian. This removes the perfect flatness of the top band. The momentum dependent Hamiltonian matrix $\mathcal{H}'(\vec{k})$ corresponding to next-nearest neighbor hopping reads

$$\mathcal{H}'(\vec{k}) = -t' \begin{bmatrix} 0 & T_1^* + T_2^* & T_2 + T_1^* T_2^* \\ T_1 + T_2 & 0 & T_1^* + T_1 T_2 \\ T_2^* + T_1 T_2 & T_1 + T_1^* T_2^* & 0 \end{bmatrix}. \tag{A.43}$$

In Section 9.4.2 we have intruced the matrix functions Λ_i which act on the sublattice degree of freedom and which are generalizations of the Pauli-matrices τ^i. They are 3×3 matrices and constitute the set of matrices spanning the space of Hermitian matrices, known as the Gell-Mann matices. Explicitly they read

$$\begin{gathered} \Lambda_{1a} = \begin{bmatrix} 0 & 1 & 0 \\ 1 & 0 & 0 \\ 0 & 0 & 0 \end{bmatrix}, \ \Lambda_{2a} = \begin{bmatrix} 0 & 0 & 0 \\ 0 & 0 & 1 \\ 0 & 1 & 0 \end{bmatrix}, \ \Lambda_{3a} = \begin{bmatrix} 0 & 0 & 1 \\ 0 & 0 & 0 \\ 1 & 0 & 0 \end{bmatrix} \\ \Lambda_{1b} = \begin{bmatrix} 0 & -i & 0 \\ i & 0 & 0 \\ 0 & 0 & 0 \end{bmatrix}, \ \Lambda_{2b} = \begin{bmatrix} 0 & 0 & 0 \\ 0 & 0 & -i \\ 0 & i & 0 \end{bmatrix}, \ \Lambda_{3b} = \begin{bmatrix} 0 & 0 & i \\ 0 & 0 & 0 \\ -i & 0 & 0 \end{bmatrix} \\ \Lambda_{1c} = \frac{1}{\sqrt{3}} \begin{bmatrix} 1 & 0 & 0 \\ 0 & 1 & 0 \\ 0 & 0 & -2 \end{bmatrix}, \ \Lambda_{2c} = \begin{bmatrix} 1 & 0 & 0 \\ 0 & -1 & 0 \\ 0 & 0 & 0 \end{bmatrix}. \end{gathered} \tag{A.44}$$

The first two sets, $\vec{\Lambda}_a$ and $\vec{\Lambda}_b$ correspond to bond ordered states as they connect different sublattices, while the third set $\vec{\Lambda}_c$ represents nontrivial charge order. Their symmetry properties are summarized and discussed in Section 9.4.2.

A.4.1 Low-energy theory and symmetry of Dirac matrices

The kagome lattice allows for two different types of low-energy description, depending on filling. As was mentioned in the main text (see Section 9.4.2), at filling $n = 1/3$ the spectrum is equivalent to that of the honeycomb lattice with conic degeneracies at the Dirac points $\vec{K}_\pm$. These isolated band touchings can be described by a Dirac theory fully analogous to the honeycomb lattice by projecting the linearly expanded Hamiltonian onto the eigenstates at $\vec{K}_\pm$, which we denote as $|+, j\rangle$ and $|-, j\rangle$ ($j = 1, 2$) for $\vec{K}_+$ and $\vec{K}_-$, respectively. Then, in the basis

$$\hat{\Phi}(\vec{q}) = \begin{bmatrix} \hat{\psi}_1(\vec{K}_+ + \vec{q}) \\ \hat{\psi}_2(\vec{K}_+ + \vec{q}) \\ \hat{\psi}_1(\vec{K}_- + \vec{q}) \\ \hat{\psi}_2(\vec{K}_- + \vec{q}) \end{bmatrix}. \tag{A.45}$$

one can obtain the same low-energy Hamiltonian as the one corresponding to the honeycomb lattice Dirac points,

$$\mathcal{H}(\vec{q}) = \hbar v_F \nu^3 \vec{q} \cdot \vec{\tau}, \tag{A.46}$$

of course for a proper choice of $|\pm, j\rangle$. Here the set of Pauli matrices ν^i acts on the valley degree ($\pm$) of freedom and the τ^i matrices on the "sublattice" degree of freedom labeled by j. Note that $v_F = \sqrt{3}at/\hbar$.

We now proceed to derive the lattice symmetry transformation properties of the low-energy Dirac matrices. To this end, we first derive the action of the generators of the group C_{6v}''' on the spinor

$$\underline{\hat{\chi}} \equiv \begin{bmatrix} \hat{\chi}_{j1} \\ \hat{\chi}_{j2} \end{bmatrix} = \begin{bmatrix} \hat{\psi}_j(\vec{K}_+) \\ \hat{\psi}_j(\vec{K}_-) \end{bmatrix}, \tag{A.47}$$

and then project that action into the low-energy subspace. Following the standard recepy described in Section 9.1, it is straightforward to dedude that the translation operator $T(\vec{x}_1)$ acts as

$$T(\vec{x}_1) \quad \rightarrow \quad \begin{bmatrix} \omega & & & & & & \\ & \omega & & & & & \\ & & \omega & & & & \\ & & & \omega^{-1} & & & \\ & & & & \omega^{-1} & & \\ & & & & & \omega^{-1} & \end{bmatrix} \underline{\hat{\chi}}, \tag{A.48}$$

(again $\omega = e^{2\pi i/3}$) while the six-fold rotation C_6 acts as

$$C_6 \quad \rightarrow \quad \begin{bmatrix} & & & & & 1 \\ & & & \omega^{-1} & & \\ & & & & \omega & \\ & & 1 & & & \\ \omega & & & & & \\ & \omega^{-1} & & & & \end{bmatrix} \underline{\hat{\chi}}, \tag{A.49}$$

note that this is diagonal in valley space as the six-fold rotation exchanges $\vec{K}_\pm$. The reflection σ_v acts as

$$\sigma_v \quad \rightarrow \quad \begin{bmatrix} & \omega^{-1} & & & & \\ \omega & & & & & \\ & & 1 & & & \\ & & & & \omega & \\ & & & \omega^{-1} & & \\ & & & & & 1 \end{bmatrix} \underline{\hat{\chi}}. \tag{A.50}$$

In order to evaluate the symmetry properties of the Dirac matrices $\nu^i\tau^j$ we need to project the 6×6 matrices given above into the low-energy subspace spanned by $|\pm, j\rangle$. If $U_\pm$ are the matrices that contain the eigenvectors of $\mathcal{H}(\vec{K}_\pm)$ in their column, we construct the matrix $U = \mathrm{Diag}(U_+, U_-)$ and evaluate $U^\dagger V U$, where V is a matrix of equation (A.51) and (A.53). Reading off the low-energy blocks from $U^\dagger V U$ yields for the translation

$$T(\vec{x}_1) \quad \rightarrow \quad \begin{bmatrix} \omega & & & & \\ & \omega & & & \\ & & \omega^{-1} & & \\ & & & \omega^{-1} & \end{bmatrix} \hat{\Phi}, \tag{A.51}$$

while the six-fold rotation C_6 takes the form

$$C_6 \quad \rightarrow \quad \begin{bmatrix} & & 1 & & \\ & & & \omega^{-1} & \\ \omega & & & & \\ & 1 & & & \end{bmatrix} \hat{\Phi}, \tag{A.52}$$

note that this is off-diagonal in valley space as the six-fold rotation exchanges $\vec{K}_\pm$. The reflection σ_v acts as

$$\sigma_v \quad \rightarrow \quad \tau^1 \hat{\chi}. \tag{A.53}$$

Time-reversal only exchanges $\vec{K}_+ \leftrightarrow \vec{K}_-$ and is thus easily seen to be represented in the low-energy subspace as

$$\mathcal{T} \quad \rightarrow \quad \mathcal{K}\nu^1\hat{\Phi}, \tag{A.54}$$

where $\mathcal{K}$ denotes complex conjugation.

This representation is very similar to and for some operations coincides with the representation of the extended point group derived for the honeucomb lattice. This is not all that surprising since the lattices are closely related. A consequence of the similarity of the representations is that we find the transformation properties of the Dirac matrices precisely coincide with those of honeycomb lattice in the chiral representation. These were summarized in Table A.1 and we refer the reader to the second of the two rows. The chiral representation is applicable here since we have chosen the eigenstates $|\pm, j\rangle$ accordingly. This concludes the discussion of the transformation properties of Dirac matrices in case of the kagome lattice.

APPENDIX B

LATTICE FERMIONS IN MAGNETIC FIELDS

B.1 Magnetic translation algebra on the lattice

In this appendix we present some details of lattice fermions models in a magnetic field. We specify the lattice sites of the square lattice by $\vec{n} = (n_x, n_y) \in \mathbb{Z}^2$. The Hamiltonian for the triangular lattice in a square geometry is given by

$$\hat{H} = \hat{T}_x + \hat{T}_y + \hat{T}_{x+y} + \text{hc}, \tag{B.1}$$

where the translation operators $\hat{T}_i$ are given by

$$\hat{T}_i = \sum_{\vec{n}} \hat{\psi}^\dagger(\vec{n} + \vec{u}_i) e^{i\theta^i(\vec{n})} \hat{\psi}(\vec{n}). \tag{B.2}$$

The presence of the compact lattice vector potential $\theta^i(\vec{n})$ represents the magnetic field. In lattice gauge theory these (exponentiated) objects are sometimes referred to as link variables, i.e. $U_{ij} = e^{ia_{ij}}$. We choose to work with the representation $\theta^i(\vec{n})$, which is related to the continuum vector potential $\vec{A}$ as

$$\theta^i(\vec{n}) = \frac{e}{\hbar} \int_{\vec{n}}^{\vec{n}+\vec{u}_i} \vec{A} \cdot d\vec{l}. \tag{B.3}$$

One may observe the identification $a_{\vec{n}+\vec{u}_i,\vec{n}} = \theta^i(\vec{n})$. Note that we write $\vec{u}_i$ to indicate a unit vector in the i-direction. The lattice field strength for a square plaquette is give by

$$\nabla_{\vec{n}} \times \theta = \theta^x(\vec{n}) + \theta^y(\vec{n}+\vec{u}_x) - \theta^x(\vec{n}+\vec{u}_y) - \theta^y(\vec{n}) = 2\pi\phi. \tag{B.4}$$

Calculating the field strength for the elementary triangles allows for an expression of $\theta^{x+y}(\vec{n})$ in terms of $\theta^x(\vec{n})$ and $\theta^y(\vec{n})$,

$$\begin{aligned} \pi\phi &= \theta^x(\vec{n}) + \theta^y(\vec{n}+\vec{u}_x) - \theta^{x+y}(\vec{n}) \\ &= \theta^{x+y}(\vec{n}) - \theta^x(\vec{n}+\vec{u}_y) - \theta^y(\vec{n}), \end{aligned} \tag{B.5}$$

from which one immediately obtains

$$\begin{aligned} \theta^{x+y}(\vec{n}) &= \theta^x(\vec{n}) + \theta^y(\vec{n}+\vec{u}_x) - \pi\phi \\ &= \theta^x(\vec{n}+\vec{u}_y) + \theta^y(\vec{n}) + \pi\phi \end{aligned} \tag{B.6}$$

It is a straightforward matter to show that $\hat{T}_x$ and $\hat{T}_y$ do not commute, but in fact satisfy

$$\hat{T}_y\hat{T}_x = e^{i2\pi\phi}\hat{T}_x\hat{T}_y. \tag{B.7}$$

The is the lattice analog of the noncommutative nature of translation operators in the continuum which is discussed in Chapter 1. Neither $\hat{T}_x$ nor $\hat{T}_y$ commute with the Hamiltonian and we wish to find translation operators that do commute with the Hamiltonian, generally given by

$$\begin{aligned} \overline{T}_x &= \sum_{\vec{n}} \hat{\psi}^\dagger(\vec{n}+\vec{u}_x)e^{i\chi^x(\vec{n})}\hat{\psi}(\vec{n}) \\ \overline{T}_y &= \sum_{\vec{n}} \hat{\psi}^\dagger(\vec{n}+\vec{u}_y)e^{i\chi^y(\vec{n})}\hat{\psi}(\vec{n}). \end{aligned} \tag{B.8}$$

By explicitly demanding that the following commutators vanish

$$[\overline{T}_x, \hat{T}_x] = [\overline{T}_x, \hat{T}_y] = [\overline{T}_x, \hat{T}_{x+y}] = 0, \tag{B.9}$$

one obtains expressions for $\chi^i(\vec{n})$ as

$$\begin{aligned} \chi^x(\vec{n}) &= \theta^x(\vec{n}) + 2\pi\phi n_y \\ \chi^y(\vec{n}) &= \theta^y(\vec{n}) - 2\pi\phi n_x. \end{aligned} \tag{B.10}$$

Even though these translation operators commute with the Hamiltonian, the do not commute between themselves,

$$[\overline{T}_x, \overline{T}_y] \neq 0. \tag{B.11}$$

One finds that instead they obey (in the Landau gauge, see below)

$$\overline{T}_x \overline{T}_y = e^{i2\pi\phi} \overline{T}_y \overline{T}_x. \tag{B.12}$$

If the flux ϕ is rational and given by p/q, p and q being relatively prime, then one finds

$$\overline{T}_x^q \overline{T}_y = e^{i2q\pi\phi} \overline{T}_y \overline{T}_x^q = \overline{T}_y \overline{T}_x^q. \tag{B.13}$$

(note that the asymmetry of $\overline{T}_x$ and $\overline{T}_x$ in this expression is due to the gauge choice). Hence, the operators $\overline{T}_x^q$ and $\overline{T}_x$ commute between themselves and the Hamiltonian and can acquire quantum numbers under the Hamiltonian.

B.2 Diagonalization of the Hamiltonian

In order to diagonalize the Hamiltonian we first need to specify a gauge. Two gauge choices will be discussed here, the Landau gauge, often the gauge of choice in the continuum, and the symmetric gauge. The Landau gauge, in the continuum and its lattice equivalent, is written as

$$\vec{A} = Bx\vec{u}_y, \quad \theta^x(\vec{n}) = 0,\ \theta^y(\vec{n}) = 2\pi\phi n_x, \tag{B.14}$$

whereas the symmetric gauge takes the form

$$\vec{A} = \frac{B}{2}(x\vec{u}_y - y\vec{u}_x), \quad \theta^x(\vec{n}) = -\pi\phi n_y,\ \theta^y(\vec{n}) = \pi\phi n_x \tag{B.15}$$

We treat the Landau gauge first. Fourier transforming yields

$$\hat{\psi}(\vec{p}) = \frac{1}{\sqrt{N_x N_y}} \sum_{\vec{n}} e^{-i(p_x n_x + p_y n_y)} \hat{\psi}(\vec{n}). \tag{B.16}$$

where N_i is the number of lattice sites in the i direction and $\vec{p}$ is the lattice momentum. The momentum is defined as $N_i p_i \in [0, 2\pi, 4\pi, \ldots, N_i 2\pi)$. The Hamiltonian in the Landau gauge takes the form

$$\hat{H} = -t \sum_{\vec{n},\vec{n'}} \hat{\psi}^\dagger(\vec{n}') \mathcal{M}_{\vec{n}'\vec{n}} \hat{\psi}(\vec{n}) + \text{hc} \tag{B.17}$$

with the matrix $\mathcal{M}_{\vec{n}'\vec{n}}$ defined as

$$\mathcal{M}_{\vec{n}'\vec{n}} = \delta_{\vec{n}',\vec{n}+\vec{u}_x} + \delta_{\vec{n}',\vec{n}+\vec{u}_y} e^{i2\pi\phi n_x} + \delta_{\vec{n}',\vec{n}+\vec{u}_x+\vec{u}_y} e^{i2\pi\phi(n_x+1/2)} \tag{B.18}$$

which becomes in momentum space

$$\hat{H} = -t \sum_{\vec{p},\vec{p}'} \hat{\psi}^\dagger(\vec{p}') \mathcal{M}_{\vec{p}'\vec{p}} \hat{\psi}(\vec{p}) + \text{hc} \tag{B.19}$$

with the momentum space matrix $\mathcal{M}_{\vec{p}'\vec{p}}$ defined as

$$\mathcal{M}_{\vec{p}'\vec{p}} = e^{-ip_x}\delta_{\vec{p}',\vec{p}} + (e^{-ip_y} + e^{i\pi\phi}e^{-i(p_x+p_y)})\delta_{p'_x,p_x+2\pi\phi}\delta_{p'_y,p_y}. \tag{B.20}$$

It is clear the Fourier transforming does not diagonalize the Hamitonian, as different momentum sectors are still coupled due to $\delta_{p'_x,p_x+2\pi\phi}$. Remembering that $\phi = p/q$ we can remedy this by defining $(k_x + 2\pi\phi j, k_y) = (p_x, p_y)$ with $j = 0, \ldots, q-1$ and at the same time make $\hat{\psi}(k_x + 2\pi\phi j, k_y) \equiv \hat{\psi}_j(k_x, k_y) = \hat{\psi}_j(\vec{k})$. This amounts to making the Brillouin zone q times smaller in the x direction, while making the real space unit cell q times larger. We note is passing that this only works if and only if p and q are relatively prime, as only in this case the prescription $(k_x + 2\pi\phi j, k_y) = (p_x, p_y)$ allows to access the full range $0 \leq p_x < 2\pi$. The $\mathcal{M}$ matrix is rewritten as

$$\begin{aligned} \mathcal{M}^{j'j}_{\vec{k}'\vec{k}} &= \mathcal{M}^{j'j}\delta_{\vec{k}',\vec{k}} \\ \mathcal{M}^{j'j} &= e^{-i(k_x+2\pi\phi j)}\delta_{j',j} + (e^{-ik_y} + e^{i\pi\phi(1-2j)}e^{-i(k_x+k_y)})\delta_{j',j+1} \end{aligned} \tag{B.21}$$

with Hamiltonian

$$\hat{H} = -t \sum_{\vec{k},j,j'} \hat{\psi}^\dagger_{j'}(\vec{k}) \mathcal{M}^{j'j} \hat{\psi}_j(\vec{k}) + \text{hc} \equiv -t \sum_{\vec{k},j,j'} \hat{\psi}^\dagger_{j'}(\vec{k}) \mathcal{H}^{j'j}(\vec{k}) \hat{\psi}_j(\vec{k}) \tag{B.22}$$

At this point we particularize to the situation $\phi = 1/2$, which is the relevant case for the Chern insulator model discussed in this thesis. We have values $j = 0, 1$ and it is a simple matter to show that in this basis one has

$$\mathcal{H}(\vec{k}) = -2t\cos k_x \tau^3 - 2t\cos k_y \tau^1 + 2t\cos(k_x + k_y)\tau^2 \tag{B.23}$$

In general, the magnetic Brillouin zone is restricted to $0 \leq k_x < 2\pi/q$ as a consequence of the folding expressed in $(k_x + 2\pi\phi j, k_y) = (p_x, p_y)$, meaning that the reciprocal lattice vector in the x direction is $\vec{G}_1 = (2\pi/q, 0)$. The example of $\phi = 1/2$ shows that the Hamiltonian as written in B.23 does *not* satisfy $\mathcal{H}(\vec{k} + \vec{G}_1) = \mathcal{H}(\vec{k})$.

This is easy to understand by looking at how the field operators respond to a shift by $\vec{G}_1$ in momentum space.

$$\begin{aligned}\hat{\psi}_j(\vec{k}+\vec{G}_1) &= \hat{\psi}(k_x+2\pi/q+2\pi\phi j, k_y)\\ &= \hat{\psi}(k_x+2\pi(pj+1)/q, k_y)\\ &= \hat{\psi}(k_x+2\pi\phi j', k_y)\end{aligned} \tag{B.24}$$

where j' and j are related by $(pj+1) \bmod q = pj' \bmod q$, or $p(j'-j)-1 = 0 \bmod q$. An example is illustrative and we take $\phi = p/q = 3/5$. It may be verified that $j = 0$ is mapped to $j = 2$, $j = 1$ to $j = 3$, $j = 2$ to $j = 4$, $j = 3$ to $j = 0$ and $j = 4$ to $j = 1$. Collecting the $\hat{\psi}_j(\vec{k})$ in the vector operator $\hat{\Psi}(\vec{k})$, we have the general relation

$$\hat{\Psi}(\vec{k}+\vec{G}_1) = U^\dagger \hat{\Psi}(\vec{k}). \tag{B.25}$$

The matrix $U^\dagger$ effectively operates as a translation operator of the index j by an amount j_Δ given by the solution of $pj_\Delta - 1 = 0 \bmod q$. Note that periodic boundary conditions apply. The eigenvalues of a translation operator are given by $e^{i2\pi j_\Delta l/q}$, with $l \in [0, 1, \ldots, q-1)$. If V is the matrix that diagonalizes $U^\dagger$ such that $V^\dagger U^\dagger V = D$ with D a diagonal matrix with the eigenvalues on the diagonal, then we have the relation

$$\hat{\Phi}(\vec{k}+\vec{G}_1) = D\hat{\Phi}(\vec{k}) \tag{B.26}$$

where $\hat{\Phi}(\vec{k}) = V^\dagger \hat{\Psi}(\vec{k})$, which is the first part of the gauge transformation on the state operators. The second part is achieved by defining a new matrix $D(\vec{k}) = \text{Diag}(d_1, \ldots, d_q)$, with $d_l = e^{ik_x l}$. We observe that $D(\vec{G}_1) = D$, which we use to define $D^\dagger(\vec{k})\hat{\Phi}(\vec{k})$, which is invariant under $\vec{k} \to \vec{k} + \vec{G}_1$. Hence, we obtain a Hamiltonian obeying $\tilde{\mathcal{H}}(\vec{k}+\vec{G}_1) = \tilde{\mathcal{H}}(\vec{k})$ by defining

$$\tilde{\mathcal{H}}(\vec{k}) = D^\dagger(\vec{k}) V^\dagger \mathcal{H}(\vec{k}) V D(\vec{k}) \tag{B.27}$$

For the particular case of $\phi = 1/2$ this amounts to

$$V = e^{-i\pi\tau^2/4}, \qquad D(\vec{k}) = \begin{bmatrix} 1 & \\ & e^{ik_x} \end{bmatrix}, \tag{B.28}$$

which yields $V^\dagger\tau^1 V = \tau^3$, $V^\dagger\tau^2 V = \tau^2$ and $V^\dagger\tau^3 V = -\tau^1$. It is straightforward to use these relations to obtain the transformed Hamiltonian.

We proceed to discuss the case of the symmetric gauge in a similar fashion. Again we write the Hamiltonian using the matrix $\mathcal{M}$ and obtain

$$\mathcal{M}_{\vec{n}'\vec{n}} = \delta_{\vec{n}',\vec{n}+\vec{u}_x} e^{-i\pi\phi n_y} + \delta_{\vec{n}',\vec{n}+\vec{u}_y} e^{i\pi\phi n_x} + \delta_{\vec{n}',\vec{n}+\vec{u}_x+\vec{u}_y} e^{i\pi\phi(n_x-n_y)} \tag{B.29}$$

Using the same Fourier transform as before one derives in momentum space

$$\hat{H} = -t \sum_{\vec{p},\vec{p}'} \hat{\psi}^{\dagger}(\vec{p}') \mathcal{M}_{\vec{p}'\vec{p}} \hat{\psi}(\vec{p}) + \text{hc} \tag{B.30}$$

with the momentum space matrix $\mathcal{M}_{\vec{p}'\vec{p}}$ defined as

$$\begin{aligned} \mathcal{M}_{\vec{p}'\vec{p}} = e^{-ip_x} \delta_{p'_x,p_x} \delta_{p'_y,p_y-\pi\phi} + e^{-ip_y} \delta_{p'_x,p_x+\pi\phi} \delta_{p'_y,p_y} \\ + e^{-i(p_x+p_y)} \delta_{p'_x,p_x+\pi\phi} \delta_{p'_y,p_y-\pi\phi}. \end{aligned} \tag{B.31}$$

Since we still have $\phi = p/q$ we are forced to fold the Brillouin zone according to the rule $(k_x + \pi\phi j_x, k_y + \pi\phi j_y) = (p_x, p_y)$, which amounts to a magentic Brillouin zone given by $0 \leq k_x < \pi/q$ and $0 \leq k_y < \pi/q$. Substituting the definition of these new momenta into the matrix of equation (B.2), we derive

$$\begin{aligned} \mathcal{M}^{j'j}_{\vec{k}'\vec{k}} = \mathcal{M}^{j'j} \delta_{\vec{k}'\vec{k}} = \delta_{\vec{k}'\vec{k}} \Big(e^{-ik_x} e^{-i\pi\phi j_x} \delta_{j'_x,j_x} \delta_{j'_y,j_y-1} + \\ e^{-ik_y} e^{-i\pi\phi j_y} \delta_{j'_x,j_x+1} \delta_{j'_y,j_y} + e^{-i(k_x+k_y)} e^{-i\pi\phi(j_x+j_y)} \delta_{j'_x,j_x+1} \delta_{j'_y,j_y-1} \Big), \end{aligned} \tag{B.32}$$

where we have written j to denote the double index (j_x, j_y). The label j takes values in $j \in [0, 1, \ldots, 2q \times 2q - 1)$, which means that we have considerably increased the dimensionality of the of the state operator $\hat{\Psi}(\vec{k}) = \hat{\psi}_j(\vec{k})$ as compared to the Landau gauge.

APPENDIX C

BASIC ELEMENTS OF GROUP THEORY

The purpose of this appendix is to collect and summarize all the basic elements of group theory required to follow and understand the symmetry analysis presented in the main text. The following brief overview is therefore far from exhaustive, but it serves to introduce notation and the main concepts, in particular the extended point groups.

The group of all symmetry operations leaving a given Bravais lattice invariant is the space group S. It consists of all translations T, an Abelian subgroup of S, and the point group G. The point group can be viewed as the factor group of the space group, i.e. $G = S/T$. Throughout this work we denote general point group elements by R, meaning that $R \in G$. Translations over a lattice vector $\vec{x}$ [see equation (**??**)] are written as $T(\vec{x})$. The translation subgroup T is generated by two elements, which are $T(\vec{x}_1)$ and $T(\vec{x}_2)$ corresponding to the two lattice vectors $\vec{x}_1$ and $\vec{x}_2$. The point group G, which for our purposes is always C_{nv} with n generally beig either 4 or 6, is generated by two elements. These are the n-fold rotation C_n and the reflection σ_v. The relfection σ_v is always taken as the operations which reflects in the x-axis, i.e. $(x, y) \to (x, -y)$. Any element $R \in G$ can then be written as $R = C_n^{m_1}\sigma_v^{m_2}$. Consequently, the space group S is generated by lements $T(\vec{x}_2)^{m_4}T(\vec{x}_1)^{m_3}C_6^{m_2}\sigma_v^{m_1}$. Note that point group operations and translations do not commute, but instead satisfy $T(\vec{x})R = RT(R\vec{x})$.

In the main text we exclusively talk about the point groups C_{nv}. For spinless particles in $2D$ these groups are exactly equivalent to D_n, which are groups generated

by the n-fold rotation C_n and a non-commuting two-fold rotation C_2' around the x-axis. Hence, C_2' takes the place of σ_v, leaving all algebraic relations invariant. Below we comment on the distinction between C_{nv} and D_6 in the presence of the electron spin.

C.1 Translational symmetry breaking and "extended" point groups

The central theme of this work is interaction-induced translational symmetry breaking. In particular we have classified translational symmetry broken site, bond and flux ordered states based on lattice symmetries. Translational symmetry breaking removes a subset of translations from the full group of translations T, leading to reduced group of invariant translations which we denote as $\widetilde{T}$. Having estabslished this new group of invariant translations (which is smaller than T), we can take the space group and again calculate the point by $\widetilde{G} = S/\widetilde{T}$. The point group $\widetilde{G}$ is larger than G, as it contains elements of T no longer part of $\widetilde{T}$. In particular, if $t_1 \equiv T(\vec{x}_1)$ is no longer part of $\widetilde{T}$, it belongs to the extended point group $\widetilde{G}$.

Both for the case of the square and the hexagonal Bravais lattice we consider translational symmetry breaking such that $\widetilde{T}$ is generated by $T(2\vec{x}_1)$ and $T(2\vec{x}_2)$. This means that $T(\vec{x}_1) = t_1$, $T(\vec{x}_2) = t_2$ and $T(\vec{x}_1 + \vec{x}_2) = t_3$ are added to the point group. To illustrate this more clearly, let us take the hexagonal group C_{6v} as an example. This group has 12 elements, but the group C_{6v}''' (three primes indicate three broken elmentary translations), which also contains $t_{1,2,3}$, contains 48 elements, i.e. $48 = 12 + 3 \times 12$. Algebraic properties of these elements can be worked out using $T(\vec{x})R = RT(R\vec{x})$ and the fact that $t_i t_j = |\epsilon_{ijk}| t_k$. In particular, the conjugacy classes of the group C_{6v}''' can be calculated and the character table can be obtained in the standard way. As the point group C_{6v} is a proper subgroup of C_{6v}''' all irreducible representations of C_{6v} will also appear as irreducible representations of C_{6v}''', in addition to new irreducible representations originating from the nontrivial translations. The character tables of the groups C_{6v}''' (hexagonal) and C_{4v}''' (square) are given in Table C.6 and Table C.7, respectively. They can the used in the standard way to decompose any representation into irreducible representations.

A distinct extended point group is obtained if we anticipate translational symmetry breaking of a hexagonal lattice which triples the unit cell. In that case the translations $T(\vec{x}_1) = t_1$, $T(\vec{x}_1 + \vec{x}_2) = t_2$ (redefining the t_i) are added to the point group, leading to the group C_{6v}''. The procedure for obtaining the character table is exactly the same, however one should be careful to implement the correct algebraic relations between these t_1 and t_2. Specifically, they are each others inverse. The

Point group C_{2v}			I	C_2	σ_v	σ_v'
x^2+y^2, z^2	z	A_1	1	1	1	1
xy	L_z	A_2	1	1	-1	-1
xz	R_y, x	B_1	1	-1	1	-1
yz	R_x, y	B_2	1	-1	-1	1

Table C.1: Character table of the point group C_{2v}.

character table of C_{6v}'' is given in Table C.5.

C.2 The point groups C_{4v} and C_{6v}

In the main text we discuss square and hexagonal lattice systems. The square lattice systems have symmetry group C_{4v}, while the hexagonal lattices have point group C_{6v}. We have already mentioned that each of these groups can be generated by two elements. In case of C_{4v} these are C_4 and σ_v. All other point group operations can be written in terms of these generators as follows

$$\begin{gathered} C_2 = C_4^2, \quad C_4^{-1} = C_4^3, \\ \sigma_{v1} = \sigma_v, \quad \sigma_{v2} = C_2\sigma_v \quad \sigma_{d1} = C_4\sigma_v, \quad \sigma_{d2} = C_4^{-1}\sigma_v. \end{gathered} \tag{C.1}$$

These operations are graphically shown on the left side of Fig. C.1.

In case of C_{6v} the generators of the group are C_6 and σ_v. The other point group operations can be written in terms of them as

$$\begin{gathered} C_3 = C_6^2, \quad C_2 = C_6^3, \quad C_3^{-1} = C_6^4, \quad C_6^{-1} = C_6^5, \\ \sigma_{v1} = \sigma_v, \quad \sigma_{v2} = C_3\sigma_v \quad \sigma_{v3} = C_3^{-1}\sigma_v, \\ \sigma_{d1} = C_6\sigma_v, \quad \sigma_{d2} = C_2\sigma_v \quad \sigma_{d3} = C_6^{-1}\sigma_v. \end{gathered} \tag{C.2}$$

These operations are shown in Fig. C.1 as well, on the right side.

We note again that if we exchange σ_v and C_2', i.e. a rotation of π around the x-axis instead of a reflection, but keep the algebraic structure of group elements defined in (C.1) and (C.2) then we obtain the (dihedral) groups D_4 and D_6. The irreduble representations of C_{4v} and C_{6v} are listed in the character tables of Table C.1, C.1, C.3, and C.4.

Point group C_{4v}			I	C_2	$2C_4$	$2\sigma_v$	$2\sigma_d$
x^2+y^2, z^2	z	A_1	1	1	1	1	1
	L_z	A_2	1	1	1	-1	-1
x^2-y^2		B_1	1	1	-1	1	-1
xy		B_2	1	1	-1	-1	1
(xz, yz)	(x, y) (L_x, L_y)	E	2	-2	0	0	0

Table C.2: Character table of the point group C_{4v}.

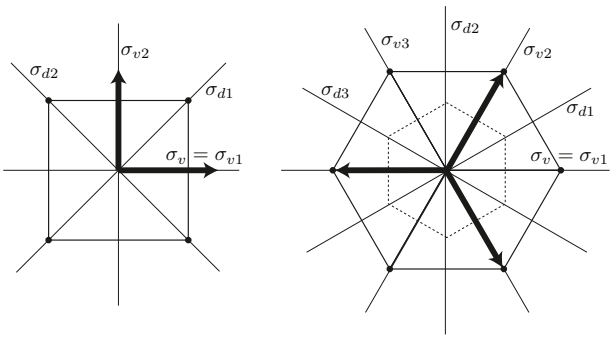

Figure C.1: Graphical representation of the point group symmetries of $2D$ square lattices (left) and hexagonal lattices (right). The reflections are given in terms of the generators $C_{4,6}$ and σ_v in the text of the present appendix.

C.2.1 M-point representation of hexagonal symmetry operations

In Section 9.4.1 we have introduced a particular representation of the hexagonal symmetry groups which proved very helpful in deriving condensate functions transforming as irreducible representations. Here we come back to this representations and provide some additional details, such as commutation relations for various elements.

The representation is defined by the actions of the rotations, reflections, and translations on the the linearly independent functions $\cos(\vec{Q}_\mu \cdot \vec{x})$, where $\vec{Q}_\mu$ ($\mu = 1, 2, 3$) are the three M-point vectors. The are collected in the 3-dimensional vector $\vec{\xi} = \xi_\mu(\vec{x}) = \cos(\vec{Q}_\mu \cdot \vec{x})$. As was shown in Section 9.4.1, we can obtain a representation of the lattice symmetry group by considering the effect of all lattice operations on the vector $\vec{\xi}$. Taking the translations, the effect of which is given by $\xi_\mu(\vec{x} + \vec{x}_j)$, we find three matrices G_j ($j = 1, 2, 3$) corresponding to $\vec{x}_j$, such that

Point group C_{3v}			I	$2C_3$	$3\sigma_v$
x^2+y^2, z^2	z	A_1	1	1	1
	L_z	A_2	1	1	-1
(xz, yz) (x^2-y^2, xy)	(x, y) (L_x, L_y)	E	2	-1	0

Table C.3: Character table of the point group C_{3v}.

Point group C_{6v}			I	C_2	$2C_3$	$2C_6$	$3\sigma_d$	$3\sigma_v$
x^2+y^2, z^2	z	A_1	1	1	1	1	1	1
	L_z	A_2	1	1	1	1	-1	-1
		B_1	1	-1	1	-1	-1	1
		B_2	1	-1	1	-1	1	-1
(xz, yz)	(x, y) (L_x, L_y)	E_1	2	-2	-1	1	0	0
(x^2-y^2, xy)		E_2	2	2	-1	-1	0	0

Table C.4: Character table of the point group C_{6v}.

$\xi_\mu(\vec{x}+\vec{x}_j) = [G_j]_{\mu\nu}\xi_\nu(\vec{x})$. Hence, for a given translation the effect on $\vec{\xi}$ is given by G_j, i.e. $G_j\vec{\xi}$. The three matrices take the form

$$G_1 = \begin{bmatrix} -1 & & \\ & -1 & \\ & & 1 \end{bmatrix},\ G_2 = \begin{bmatrix} 1 & & \\ & -1 & \\ & & -1 \end{bmatrix},\ G_3 = G_1G_2. \tag{C.3}$$

Not surprisingly, all the G_j commute, square to one, and multiplying two of them gives the third. This follows from the M-point vectors, which have the same properties under addition. Another way of understanding this is to say that M-point order implies a quadrupled real space unit cell, meaning that an even number of elementary translations must always leave the system invariant.

Regarding the point group operations, we only need the actions of the generators C_6 and σ_v on the vector ξ. In the main text we defined the matrix X to correspond to the permutation of ξ_μ as a consequence of C_6, i.e.

$$\vec{\xi}(C_6\vec{x}) = X\vec{\xi}(\vec{x}), \quad X = \begin{bmatrix} 0 & 0 & 1 \\ 1 & 0 & 0 \\ 0 & 1 & 0 \end{bmatrix} \tag{C.4}$$

Note that X has the property $X^3 = 1$ and thus $X^{-1} = X^2$. In addition the relation $X^{-1} = X^T$ holds, where X^T is the transpose. For the reflection σ_v we had defined an element Y such that

$$\vec{\xi}(\sigma_v \vec{x}) = Y\vec{\xi}(\vec{x}), \quad Y = \begin{bmatrix} 0 & 0 & 1 \\ 0 & 1 & 0 \\ 1 & 0 & 0 \end{bmatrix} \tag{C.5}$$

With the explicit matrix expression at hand it is a simple matter to show that $(XY)^2 = 1$, from which all algebraic relations between X and Y follow.

We now proceed to list some helpful algebraic commutation properties of the G_j and X. It is a simple matter to derive or check that

$$\begin{aligned} G_2X = XG_1, \quad & G_1X^{-1} = X^{-1}G_2 \\ G_1X = XG_3, \quad & G_3X^{-1} = X^{-1}G_1 \\ G_3X = XG_2, \quad & G_2X^{-1} = X^{-1}G_3. \end{aligned} \tag{C.6}$$

In the same way we have for the G_j and Y

$$\begin{aligned} G_2Y &= YG_1 \\ G_1Y &= YG_2 \\ G_3Y &= YG_3. \end{aligned} \tag{C.7}$$

We close by mentioning that the representation of C_{6v} in terms of X and Y is reducible and the decomposition is given by $A_1 \oplus E_2$. However, the elements G_j, X and Y generate a representation of C_{6v}''', which is irreducible and equal to F_1.

C.3 Symmetry properties with spin

Chapter 10 deals with spinful condensates or triplet condensates. The description of these condensates requires taking into account the point (or space) group respresenations acting on the spinor degree of freedom. In terms of equation (9.6) of the main text, one needs to consider the matrix U_R^{o} acting on the spinor degree af freedom. It is a matrix belonging to $SU(2)$.

As was already mentioned before, for spinless particles the groups C_{nv} and D_n may be considered identical, as indeed both send $(x, y) \to (x, -y)$ under the reflection (C_{nv}) in the $x - z$ plane or the twofold rotation about the x-axis (D_n). In the spinful case, there is a difference however, since reflections and rotations act in different ways. The transformation properties for the n-fold rotation about the z-axis are

Conjugacy class	$\mathcal{C}_1''$	$\mathcal{C}_2''$	$\mathcal{C}_3''$	$\mathcal{C}_4''$	$\mathcal{C}_5''$	$\mathcal{C}_6''$	$\mathcal{C}_7''$	$\mathcal{C}_8''$	$\mathcal{C}_9''$
Representative	I	t_1	C_2	C_3	t_1C_3	C_6	σ_v	$t_1\sigma_v$	σ_d
A_1	1	1	1	1	1	1	1	1	1
A_2	1	1	1	1	1	1	-1	-1	-1
B_1	1	1	-1	1	1	-1	1	1	-1
B_2	1	1	-1	1	1	-1	-1	-1	1
E_1	2	2	-2	-1	-1	1	0	0	0
E_2	2	2	2	-1	-1	-1	0	0	0
E_1'	2	-1	0	2	-1	0	2	-1	0
E_2'	2	-1	0	2	-1	0	-2	1	0
G'	4	-2	0	-2	1	0	0	0	0

Table C.5: Character table of the point group C_{6v}''. Translations t_1 and t_2 correspond to $T(\vec{x}_1)$ and $T(\vec{x}_2)$, respectively. The irreducible representations that arise as a consequence of the added translations are E_1' $(2D)$, E_2' $(2D)$ and G' $(4D)$. The conjugacy classes consist of the elements: $\mathcal{C}_1'' = \{I\}$, $\mathcal{C}_2'' = \{t_1, t_2\}$, $\mathcal{C}_3'' = \{C_2, t_iC_2\}$, $\mathcal{C}_4'' = \{C_3, C_3^{-1}\}$, $\mathcal{C}_5'' = \{t_iC_3, t_iC_3^{-1}\}$, $\mathcal{C}_6'' = \{t_iC_6, t_iC_6^{-1}, C_6, C_6^{-1}\}$, $\mathcal{C}_7'' = \{3\sigma_v\}$, $\mathcal{C}_8'' = \{3t_1\sigma_v, 3t_2\sigma_v\}$, $\mathcal{C}_9'' = \{3\sigma_d, 3t_i\sigma_d\}$.

straightforward to deduce, using the standard formula for $SU(2)$ rotations. A rotation about an axis $\hat{n}$ by an angle θ is given by

$$U = e^{-i\theta\hat{n}\cdot\vec{\sigma}/2} = \cos\frac{\theta}{2} - i\sin\frac{\theta}{2}\,\hat{n}\cdot\vec{\sigma} \tag{C.8}$$

Applying this formula to the n-fold rotations (where we take $n = 4, 6$ for definiteness), which are rotations about the z-axis, the rotation matrix becomes $e^{-i\pi\sigma^3/n}$ and the Pauli matrices transform as

$$C_n \;:\qquad \sigma^3 \;\to\; \sigma^3; \qquad \sigma^\pm \;\to\; e^{\pm i2\pi/n}\sigma^\pm \tag{C.9}$$

This is true for both C_{nv} and D_6. The distinction between the two groups comes from the reflections (C_{nv}) or the two-fold rotations (D_6). For the group D_n the two-fold rotation is also simple to write down. A rotation of π about the x-axis is given by $-i\sigma^1$ and thus we have

$$C_2' \;:\qquad \sigma^{2,3} \;\to\; -\sigma^{2,3}; \qquad \sigma^1 \;\to\; \sigma^1 \tag{C.10}$$

For the reflection on the other we need to take into account that a magnetic moment like spin can be thought of as generated by a small current loop. A spin pointing in

the x-direction may be thought of as a current loop in the $z-y$ plane and hence a reflection in the $x-z$ plane changes the current direction. The spin will be rotated by π. One observes that the only direction that does not change is a spin pointing in the y-direction. The transformation properties follow:

$$\sigma_v \ : \qquad \sigma^{1,3} \ \rightarrow \ -\sigma^{1,3}; \qquad \sigma^2 \ \rightarrow \ \sigma^2 \tag{C.11}$$

We therefore observe that the transformation properties of the reflections and two-fold rotations differ and therefore define distinct point groups.

Another way of understanding the difference between C_{6v} is to view both C_{6v} and D_6 as subgroups of O_h, i.e. the group of all symmetries of the cube. It is known that all elements of O_h may be written as a product of a proper rotation and the inversion operation. Rotations rotate pseusovectors such as angular momentum and the electron spin, however, the inversion operation does nothing to a pseudovector. Therefore, in order to find out what member of $SU(2)$ corresponds to σ_v and C_2', one needs to find out what proper rotation make up these elements. In the first case it is a rotation about the x-axis and in the second case it is a rotation about the y-axis.

We stress here again that while details do depend on this difference in the spinful case the main conclusions reached in this work do not depend on whether the symmetry group is C_{6v} or D_6.

C.3.1 Spinful M-point representation of hexagonal symmetry operations

An important concept introduced in Chapter 10 is global rotation equivalence. For spinful condensates point group operations and translations may need to be combined with a global spin rotation in order to make them good symmetries. We have only treated spinful condensates constructed from M-point vectors in hexagonal systems and the connection between elements of C_{6v}''' and global $U(2)$ rotations (not $SU(2)$) is established via the 3×3 matrices G_j, X and Y (see Section C.2.1) acting on $\vec{\xi}$. This connection is explicitly expressed in equation (10.5) of the main text.

The mapping from the 3×3 representation, i.e. matrices which can be interpreted as rotation matrices of $O(3)$, to the space $U(2)$ preserves the algebraic structure and defines another representation, with the electron spin wavefunctions as basis functions. It is straighforward to associate a $U(2)$ matrix to an $O(3)$ rotation matrix, by determining the rotation axis and angle. For instance, the translation element G_1 corresponds to a rotation about the z-axis by π. Hence, the associated $U(2)$ matrix is

Conj. class	$\mathcal{C}_1'''$	$\mathcal{C}_2'''$	$\mathcal{C}_3'''$	$\mathcal{C}_4'''$	$\mathcal{C}_5'''$	$\mathcal{C}_6'''$	$\mathcal{C}_7'''$	$\mathcal{C}_8'''$	$\mathcal{C}_9'''$	$\mathcal{C}_{10}'''$
Repres.		t_1	C_2	t_1C_2	C_3	C_6	σ_v	$t_1\sigma_v$	σ_d	$t_1\sigma_{d1}$
A_1	1	1	1	1	1	1	1	1	1	1
A_2	1	1	1	1	1	1	−1	−1	−1	−1
B_1	1	1	−1	−1	1	−1	1	1	−1	−1
B_2	1	1	−1	−1	1	−1	−1	−1	1	1
E_1	2	2	−2	−2	−1	1	0	0	0	0
E_2	2	2	2	2	−1	−1	0	0	0	0
F_1	3	−1	3	−1	0	0	1	−1	1	−1
F_2	3	−1	3	−1	0	0	−1	1	−1	1
F_3	3	−1	−3	1	0	0	1	−1	−1	1
F_4	3	−1	−3	1	0	0	−1	1	1	−1

Table C.6: The point group C_{6v}'''. Translations t_1 and t_2 correspond to $T(\vec{x}_1)$ and $T(\vec{x}_2)$, respectively. $t_3 = T(\vec{x}_1 + \vec{x}_2)$. The irreducible representations that arise as a consequence of the added translations are F_1, F_2, F_3 and F_4, all three-dimensional. The conjugacy classes consist of the elements: $\mathcal{C}_1''' = \{I\}$, $\mathcal{C}_2''' = \{t_1, t_2, t_3\}$, $\mathcal{C}_3''' = \{C_2\}$, $\mathcal{C}_4''' = \{t_iC_2\}$, $\mathcal{C}_5''' = \{t_iC_3, t_iC_3^{-1}, C_3, C_3^{-1}\}$, $\mathcal{C}_6''' = \{t_iC_6, t_iC_6^{-1}, C_6, C_6^{-1}\}$, $\mathcal{C}_7''' = \{3\sigma_v, t_1\sigma_{v2}, t_2\sigma_{v3}, t_3\sigma_{v1}\}$, $\mathcal{C}_8''' = \{t_1\sigma_v, t_2\sigma_v, t_2\sigma_{v2}, t_3\sigma_{v2}, t_1\sigma_{v3}, t_3\sigma_{v3}\}$, $\mathcal{C}_9''' = \{3\sigma_d, t_2\sigma_{d1}, t_3\sigma_{d2}, t_1\sigma_{v3}\}$, $\mathcal{C}_{10}''' = \{t_1\sigma_{d1}, t_3\sigma_{d1}, t_1\sigma_{d2}, t_2\sigma_{d2}, t_2\sigma_{d3}, t_3\sigma_{d3}\}$.

$-i\sigma^3$. We simply find for all translations.

$$\begin{aligned} G_1 &\rightarrow e^{-i\pi\sigma^3/2} = -i\sigma^3 \\ G_2 &\rightarrow e^{-i\pi\sigma^1/2} = -i\sigma^1 \\ G_3 &\rightarrow e^{-i\pi\sigma^2/2} = -i\sigma^2. \end{aligned} \tag{C.12}$$

The matrix X, interpreted as rotation matrix, corresponds to a rotation by $2\pi/3$ about the axis $\hat{n} = (1,1,1)/\sqrt{3}$. We can decompose it into two separate rotations about the z and y-axes (Euler rotations) and obtain the $SU(2)$ matrices

$$\begin{aligned} X &\rightarrow e^{-i\pi\sigma^2/4}e^{-i\pi\sigma^3/4} \\ X^T &\rightarrow e^{i\pi\sigma^3/4}e^{i\pi\sigma^2/4}. \end{aligned} \tag{C.13}$$

Note that these are elements of $SU(2)$ since X and X^T are proper rotations. This is different for Y, which has determinant -1. Therefore $-Y$ is a proper rotation which

can be identified with an element of $SU(2)$. One finds that

$$-Y \quad \rightarrow \quad e^{i\pi\sigma^2/4}e^{-i\pi\sigma^3/2} = -ie^{i\pi\sigma^2/4}\sigma^3, \tag{C.14}$$

which completes the mapping of G_j, X and Y onto $U(2)$ matrices. This mapping is at the heart of analyzing symmetry properties of spinful condensates. In particular, the appearance of an extra minus sign for Y is what causes some reflections to constitute good symmetries in the presence of spin, as explained in Chapter 10.

Conjugacy class	$\mathcal{C}_1'''$	$\mathcal{C}_2'''$	$\mathcal{C}_3'''$	$\mathcal{C}_4'''$	$\mathcal{C}_5'''$	$\mathcal{C}_6'''$	$\mathcal{C}_7'''$	$\mathcal{C}_8'''$	$\mathcal{C}_9'''$	$\mathcal{C}_{10}'''$	$\mathcal{C}_{11}'''$	$\mathcal{C}_{12}'''$	$\mathcal{C}_{13}'''$	$\mathcal{C}_{14}'''$
Representative	I	t_1	t_3	C_2	t_1C_2	t_3C_2	C_4	t_1C_4	σ_v	$t_3\sigma_v$	$t_1\sigma_v$	$t_2\sigma_v$	σ_{d1}	$t_1\sigma_{d1}$
A_1	1	1	1	1	1	1	1	1	1	1	1	1	1	1
A_2	1	1	1	1	1	1	1	1	−1	−1	−1	−1	−1	−1
B_1	1	1	1	1	1	1	−1	−1	1	1	1	1	−1	−1
B_2	1	1	1	1	1	1	−1	−1	−1	−1	−1	−1	1	1
E_1	2	2	2	−2	−2	−2	0	0	0	0	0	0	0	0
A_1'	1	−1	1	1	−1	1	1	−1	1	−1	−1	1	1	−1
A_2'	1	−1	1	1	−1	1	1	−1	−1	1	1	−1	−1	1
B_1'	1	−1	1	1	−1	1	−1	1	1	−1	−1	1	−1	1
B_2'	1	−1	1	1	−1	1	−1	1	−1	1	1	−1	1	−1
E_1'	2	−2	2	−2	2	−2	0	0	0	0	0	0	0	0
E_2	2	0	−2	2	0	−2	0	0	−2	0	0	2	0	0
E_3	2	0	−2	2	0	−2	0	0	2	0	0	−2	0	0
E_4	2	0	−2	−2	0	2	0	0	0	2	−2	0	0	0
E_5	2	0	−2	−2	0	2	0	0	0	−2	2	0	0	0

Table C.7: Character table of the point group C_{6v}'''. Translations t_1 and t_2 correspond to $T(\vec{x}_1)$ and $T(\vec{x}_2)$, respectively. $t_3 = T(\vec{x}_1 + \vec{x}_2)$. The conjugacy classes consist of the elements: $\mathcal{C}_1''' = \{I\}$, $\mathcal{C}_2''' = \{t_1, t_2\}$, $\mathcal{C}_3''' = \{t_3\}$, $\mathcal{C}_4''' = \{C_2\}$, $\mathcal{C}_5''' = \{t_1C_2, t_2C_2\}$, $\mathcal{C}_6''' = \{t_3C_2\}$, $\mathcal{C}_7''' = \{C_4, C_4^{-1}, t_3C_4, t_3C_4^{-1}\}$, $\mathcal{C}_8''' = \{t_1C_4, t_1C_4^{-1}, t_2C_4, t_2C_4^{-1}\}$, $\mathcal{C}_9''' = \{\sigma_{v1}, \sigma_{v2}\}$, $\mathcal{C}_{10}''' = \{t_3\sigma_{v1}, t_3\sigma_{v2}\}$, $\mathcal{C}_{11}''' = \{t_1\sigma_{v1}, t_2\sigma_{v2}\}$, $\mathcal{C}_{12}''' = \{t_2\sigma_{v1}, t_1\sigma_{v2}\}$, $\mathcal{C}_{13}''' = \{\sigma_{d1}, \sigma_{d2}, t_3\sigma_{d1}, t_3\sigma_{d2}\}$ and $\mathcal{C}_{14}''' = \{t_1\sigma_{d1}, t_1\sigma_{d2}, t_2\sigma_{d1}, t_2\sigma_{d2}\}$.

BIBLIOGRAPHY

[1] C. L. Kane and E. J. Mele, Phys Rev Lett **95**, 146802 (2005).

[2] L. Fu and C. L. Kane, Phys Rev B **74**, 195312 (2006).

[3] L. Fu, C. L. Kane, and E. J. Mele, Phys Rev Lett **98**, 106803 (2007).

[4] J. E. Moore and L. Balents, Phys Rev B **75**, 121306 (2007).

[5] R. Roy, Phys Rev B **79**, 195321 (2009).

[6] B. A. Bernevig, T. L. Hughes, and S.-C. Zhang, Science **314**, 1757 (2006).

[7] M. Koenig, S. Wiedmann, C. Bruene, A. Roth, H. Buhmann, L. W. Molenkamp, X.-L. Qi, and S.-C. Zhang, Science **318**, 766 (2007).

[8] D. Hsieh, D. Qian, L. Wray, Y. Xia, Y. S. Hor, R. J. Cava, and M. Z. Hasan, Nature **452**, 970 (2008).

[9] Y. Xia, L. Wray, D. Qian, D. Hsieh, A. Pal, H. Lin, A. Bansil, D. Grauer, Y. S. Hor, R. J. Cava, and M. Z. Hasan, arXiv (2008).

[10] D. C. Tsui, H. L. Stormer, and A. C. Gossard, Phys Rev Lett **48**, 1559 (1982).

[11] X.-G. Wen, Adv Phys **44**, 405 (1995).

[12] M. Z. Hasan and C. L. Kane, Rev Mod Phys **82**, 3045 (2010).

[13] S. M. Girvin, A. H. MacDonald, and P. M. Platzman, Phys Rev Lett **54**, 581 (1985).

[14] F. D. M. Haldane, Phys Rev Lett **55**, 2095 (1985).

[15] T. Neupert, L. Santos, S. Ryu, C. Chamon, and C. Mudry, Phys Rev B **86**, 035125 (2012).

[16] D. Thouless, M. Kohmoto, M. Nightingale, and M. den Nijs, Phys Rev Lett **49**, 405 (1982).

[17] S.-C. Zhang, Int J Mod Phys B **6**, 25 (1992).

[18] G. E. Volovik, *The Universe in a Helium Droplet* (Oxford University Press, USA, 2009).

[19] W. P. Su, J. R. Schrieffer, and A. J. Heeger, Phys Rev Lett **42**, 1698 (1979).

[20] N. Furukawa, *Geometry, Topology and Physics* (Taylor and Francis, New York, 2003 (2nd edition)).

[21] A. P. Schnyder, S. Ryu, A. Furusaki, and A. W. W. Ludwig, Phys Rev B **78**, 195125 (2008).

[22] S. Ryu, A. P. Schnyder, A. Furusaki, and A. W. W. Ludwig, New J Phys **12**, 065010 (2010).

[23] C. L. Kane and E. J. Mele, Phys Rev Lett **95**, 226801 (2005).

[24] H. B. Nielsen and M. Ninomiya, Phys Lett B **130**, 389 (1983).

[25] K. Wilson, Rev Mod Phys **47**, 773 (1975).

[26] A. C. Hewson, *The Kondo Problem to Heavy Fermions* (Cambridge University Press, Cambridge, England, 1993).

[27] E. Dagotto, T. Hotta, and A. Moreo, Phys Rep **344**, 1 (2001).

[28] E. Dagotto, *Nanoscale Phase Separation and Colossal Magnetoresistance* (Springer, Berlin, 2002).

[29] R. Shindou and N. Nagaosa, Phys Rev Lett **87**, 116801 (2001).

[30] I. Martin and C. D. Batista, Phys Rev Lett **101**, 156402 (2008).

[31] Y. Akagi and Y. Motome, J Phys Soc Jpn **79**, 083711 (2010).

[32] S. Kumar and J. van den Brink, Phys Rev Lett **105**, 216405 (2010).

[33] G.-W. Chern, Phys Rev Lett **105**, 226403 (2010).

[34] Y. Motome and N. Furukawa, Phys Rev Lett **104**, 106407 (2010).

[35] M. Udagawa and R. Moessner, Phys Rev Lett **111**, 036602 (2013).

[36] M. Udagawa, H. Ishizuka, and Y. Motome, Phys Rev Lett **108**, (2012).

[37] R. Flint and T. Senthil, Phys Rev B **87**, 125147 (2013).

[38] H. J. Schulz, Phys Rev Lett **65**, 2462 (1990).

[39] Z. Y. Weng, C. Ting, and T. Lee, Phys Rev B **43**, 3790 (1991).

[40] T. Li, Epl-Europhys Lett **97**, 37001 (2012).

[41] J. Vergés, V. Martin-Mayor, and L. Brey, Phys Rev Lett **88**, 136401 (2002).

[42] S. Yunoki, A. Moreo, and E. Dagotto, Phys Rev Lett **81**, 5612 (1998).

[43] S. Kumar and P. Majumdar, Phys Rev Lett **92**, 126602 (2004).

[44] S. Kumar and P. Majumdar, Phys Rev Lett **96**, 016602 (2006).

[45] S. Kumar and P. Majumdar, Eur Phys J B **50**, 571 (2006).

[46] Z. Y. Meng, T. C. Lang, S. Wessel, F. F. Assaad, and A. Muramatsu, Nature **464**, 847 (2010).

[47] F. Wang, Phys Rev B **82**, 024419 (2010).

[48] Y.-M. Lu and Y. Ran, Phys Rev B **84**, 024420 (2011).

[49] A. Vaezi and X.-G. Wen, arXiv (2010).

[50] Y. Yafet and C. Kittel, Phys Rev **87**, 290 (1952).

[51] C. Castelnovo, R. Moessner, and S. L. Sondhi, Nature **451**, 42 (2008).

[52] J. S. Gardner, M. J. P. Gingras, and J. E. Greedan, Rev Mod Phys **82**, 53 (2010).

[53] Z. Nussinov and G. Ortiz, P Natl Acad Sci Usa **106**, 16944 (2009).

[54] B. Uchoa, T. G. Rappoport, and A. H. Castro Neto, Phys Rev Lett **106**, 016801 (2011).

[55] A. M. Black-Schaffer, Phys Rev B **81**, 205416 (2010).

[56] A. M. Black-Schaffer, Phys Rev B **82**, 073409 (2010).

[57] M. Daghofer, N. Zheng, and A. Moreo, Phys Rev B **82**, 121405 (2010).

[58] O. Smirnova, M. Azuma, N. Kumada, Y. Kusano, M. Matsuda, Y. Shimakawa, T. Takei, Y. Yonesaki, and N. Kinomura, J. Am. Chem. Soc. **131**, 8313 (2009).

[59] S. Okubo, F. Elmasry, W. Zhang, M. Fujisawa, T. Sakurai, H. Ohta, M. Azuma, O. A. Sumirnova, and N. Kumada, J. Phys.: Conf. Ser. **200**, 022042 (2010).

[60] R. Ganesh, D. N. Sheng, Y.-J. Kim, and A. Paramekanti, Phys Rev B **83**, 144414 (2011).

[61] A. Mulder, R. Ganesh, L. Capriotti, and A. Paramekanti, Phys Rev B **81**, 214419 (2010).

[62] H. C. Kandpal and J. van den Brink, Phys Rev B **83**, 140412 (2011).

[63] J. Bréger, M. Jiang, N. Dupré, Y. S. Meng, Y. Shao-Horn, G. Ceder, and C. P. Grey, Journal of Solid State Chemistry **178**, 2575 (2005).

[64] R. Yu, S. Yunoki, S. Dong, and E. Dagotto, Phys Rev B **80**, 125115 (2009).

[65] A. Mishra, M. Ma, F.-C. Zhang, S. Guertler, L.-H. Tang, and S. Wan, Phys Rev Lett **93**, 207201 (2004).

[66] M. Biskup, L. Chayes, and Z. Nussinov, Commun Math Phys **255**, 253 (2005).

[67] Z. Nussinov, M. Biskup, L. Chayes, and J. van den Brink, Europhys Lett **67**, 990 (2004).

[68] F. Trousselet, A. M. Oleś, and P. Horsch, Epl-Europhys Lett **91**, 40005 (2010).

[69] S. Liang, M. Daghofer, S. Dong, C. Şen, and E. Dagotto, Phys Rev B **84**, 024408 (2011).

[70] J. Riera, K. Hallberg, and E. Dagotto, Phys Rev Lett **79**, 713 (1997).

[71] N. Elstner, R. Singh, and A. Young, Phys Rev Lett **71**, 1629 (1993).

[72] R. Roy, Phys Rev B **79**, 195322 (2009).

[73] D. Hsieh, Y. Xia, D. Qian, L. Wray, J. H. Dil, F. Meier, J. Osterwalder, L. Patthey, J. G. Checkelsky, N. P. Ong, A. V. Fedorov, H. Lin, A. Bansil, D. Grauer, Y. S. Hor, R. J. Cava, and M. Z. Hasan, Nature **460**, 1101 (2009).

[74] Y. Xia, D. Qian, D. Hsieh, L. Wray, A. Pal, H. Lin, A. Bansil, D. Grauer, Y. S. Hor, R. J. Cava, and M. Z. Hasan, Nat Phys **5**, 398 (2009).

[75] K. von Klitzing, G. Dorda, and M. Pepper, Phys Rev Lett **45**, 494 (1980).

[76] F. D. M. Haldane, Phys Rev Lett **61**, 2015 (1988).

[77] C.-X. Liu, X.-L. Qi, X. Dai, Z. Fang, and S.-C. Zhang, Phys Rev Lett **101**, 146802 (2008).

[78] Y. Taguchi, Y. Oohara, H. Yoshizawa, N. Nagaosa, and Y. Tokura, Science **291**, 2573 (2001).

[79] Y. Machida, S. Nakatsuji, Y. Maeno, T. Tayama, T. Sakakibara, and S. Onoda, Phys Rev Lett **98**, 057203 (2007).

[80] H. Takatsu, S. Yonezawa, S. Fujimoto, and Y. Maeno, Phys Rev Lett **105**, 137201 (2010).

[81] K. K. Gomes, W. Mar, W. Ko, F. Guinea, and H. C. Manoharan, Nature **483**, 306 (2012).

[82] X.-L. Qi, Y.-S. Wu, and S.-C. Zhang, Phys Rev B **74**, 085308 (2006).

[83] H. Zhang, C. Lazo, S. Blügel, S. Heinze, and Y. Mokrousov, Phys Rev Lett **108**, 056802 (2012).

[84] S. Raghu, X.-L. Qi, C. Honerkamp, and S.-C. Zhang, Phys Rev Lett **100**, 156401 (2008).

[85] K. Ohgushi, S. Murakami, and N. Nagaosa, Phys Rev B **62**, R6065 (2000).

[86] K. Sun, H. Yao, E. S. Fradkin, and S. A. Kivelson, Phys Rev Lett **103**, 046811 (2009).

[87] K. Sun, Z.-C. Gu, H. Katsura, and S. Das Sarma, Phys Rev Lett **106**, 236803 (2011).

[88] S. Uebelacker and C. Honerkamp, Phys Rev B **84**, 205122 (2011).

[89] P. Schobinger-Papamantellos, J. Rodríguez-Carvajal, and K. H. J. Buschow, Journal of Magnetism and Magnetic Materials **310**, 63 (2007).

[90] L. D. C. Jaubert, M. Haque, and R. Moessner, Phys Rev Lett **107**, 177202 (2011).

[91] L. D. C. Jaubert, S. Piatecki, M. Haque, and R. Moessner, Phys Rev B **85**, 054425 (2012).

[92] I. Affleck and J. B. Marston, Phys Rev B **37**, 3774 (1988).

[93] J. Lorenzana, G. Seibold, C. Ortix, and M. Grilli, Phys Rev Lett **101**, 186402 (2008).

[94] M. Yamanaka, W. Koshibae, and S. Maekawa, Phys Rev Lett **81**, 5604 (1998).

[95] D. Agterberg and S. Yunoki, Phys Rev B **62**, 13816 (2000).

[96] H. Aliaga, B. Normand, K. Hallberg, M. Avignon, and B. Alascio, Phys Rev B **64**, 024422 (2001).

[97] X. Chen, S. Dong, and J. M. Liu, Phys Rev B **81**, 064420 (2010).

[98] A. H. Castro Neto, F. Guinea, N. M. R. Peres, K. S. Novoselov, and A. K. Geim, Rev Mod Phys **81**, 109 (2009).

[99] Y. Hatsugai, T. Fukui, and H. Aoki, Phys Rev B **74**, 205414 (2006).

[100] Y. Kato, I. Martin, and C. D. Batista, Phys Rev Lett **105**, 266405 (2010).

[101] M. Onoda and N. Nagaosa, J Phys Soc Jpn **71**, 19 (2002).

[102] S. Ryu, C. Mudry, C.-Y. Hou, and C. Chamon, Phys Rev B **80**, (2009).

[103] R. W. Jackiw, Phys Rev D **29**, 2375 (1984).

[104] D. N. Sheng, Z.-C. Gu, K. Sun, and L. Sheng, Nat Commun **2**, 389 (2011).

[105] N. Regnault and B. A. Bernevig, Phys. Rev. X **1**, 021014 (2011).

[106] J. W. F. Venderbos, M. Daghofer, and J. van den Brink, Phys Rev Lett **107**, 116401 (2011).

[107] J. W. F. Venderbos, S. Kourtis, J. van den Brink, and M. Daghofer, Phys Rev Lett **108**, 126405 (2012).

[108] T. Neupert, L. Santos, C. Chamon, and C. Mudry, Phys Rev Lett **106**, (2011).

[109] R. A. Muniz, A. Rahmani, and I. Martin, arXiv (2011).

[110] J. W. F. Venderbos, M. Daghofer, J. van den Brink, and S. Kumar, Phys Rev Lett **109**, 166405 (2012).

[111] X.-L. Qi and S.-C. Zhang, Rev Mod Phys **83**, 1057 (2011).

[112] C. Bruene, C. X. Liu, E. G. Novik, E. M. Hankiewicz, H. Buhmann, Y. L. Chen, X.-L. Qi, Z. X. Shen, S.-C. Zhang, and L. W. Molenkamp, Phys Rev Lett **106**, 126803 (2011).

[113] E. Tang, J.-W. Mei, and X.-G. Wen, Phys Rev Lett **106**, 236802 (2011).

[114] R. B. Laughlin, Phys Rev Lett **50**, 1395 (1983).

[115] X.-L. Qi, Phys Rev Lett **107**, 126803 (2011).

[116] Y.-L. Wu, N. Regnault, and B. A. Bernevig, Phys Rev B **86**, 085129 (2012).

[117] S. Das Sarma, M. H. Freedman, and C. Nayak, Phys Rev Lett **94**, 166802 (2005).

[118] Y. Tokura and N. Nagaosa, Science **288**, 462 (2000).

[119] Z. Fang, K. Terakura, and N. Nagaosa, New J Phys **7**, 66 (2005).

[120] G. Jackeli and G. Khaliullin, Phys Rev Lett **102**, 017205 (2009).

[121] D. Pesin and L. Balents, Nat Phys **6**, 376 (2010).

[122] J. van den Brink, G. Khaliullin, and D. Khomskii, Phys Rev Lett **83**, 5118 (1999).

[123] T. Hotta, M. Moraghebi, A. Feiguin, A. Moreo, S. Yunoki, and E. Dagotto, Phys Rev Lett **90**, 247203 (2003).

[124] H. Pen, J. van den Brink, D. Khomskii, and G. Sawatzky, Phys Rev Lett **78**, 1323 (1997).

[125] W. Koshibae and S. Maekawa, Phys Rev Lett **91**, 257003 (2003).

[126] D. J. Thouless, Phys Rev B **40**, 12034 (1989).

[127] B. A. Bernevig and S.-C. Zhang, Phys Rev Lett **96**, 106802 (2006).

[128] H. Zhang, C.-X. Liu, X.-L. Qi, X. Dai, Z. Fang, and S.-C. Zhang, Nat Phys **5**, 438 (2009).

[129] C. Nayak, S. H. Simon, A. Stern, M. H. Freedman, and S. Das Sarma, Rev Mod Phys **80**, 1083 (2008).

[130] X. Hu, M. Kargarian, and G. A. Fiete, Phys Rev B **84**, 155116 (2011).

[131] Y.-F. Wang, Z.-C. Gu, C.-D. Gong, and D. N. Sheng, Phys Rev Lett **107**, 146803 (2011).

[132] S. Nishimoto, M. Nakamura, A. O'Brien, and P. Fulde, Phys Rev Lett **104**, 196401 (2010).

[133] P. Matl, N. Ong, Y. Yan, Y. Li, D. Studebaker, T. Baum, and G. Doubinina, Phys Rev B **57**, 10248 (1998).

[134] W. A. Harrison, *Electronic Structure and Properties of Solids* (W.H. Freeman, San Francisco, 1980).

[135] J. C. Slater and G. F. Koster, Phys Rev **94**, 1498 (1954).

[136] B. Normand and A. M. Oles, Phys Rev B **78**, (2008).

[137] T. Nomura and K. Yamada, J Phys Soc Jpn **69**, 1856 (2000).

[138] F. Wilczek, Phys Rev Lett **49**, 957 (1982).

[139] F. D. M. Haldane, Phys Rev Lett **67**, 937 (1991).

[140] Y.-L. Wu, B. A. Bernevig, and N. Regnault, Phys Rev B **85**, 075116 (2012).

[141] S. Kourtis, J. W. F. Venderbos, and M. Daghofer, Phys Rev B **86**, 235118 (2012).

[142] S. A. Parameswaran, R. Roy, and S. L. Sondhi, Phys Rev B **85**, 241308 (2012).

[143] B. A. Bernevig and N. Regnault, Phys Rev B **85**, 075128 (2012).

[144] M. O. Goerbig, Eur Phys J B **85**, 15 (2012).

[145] R. Roy, arXiv (2012).

[146] Y. Hatsugai and M. Kohmoto, Phys Rev B **42**, 8282 (1990).

[147] B. A. Bernevig and T. L. Hughes, *Topological Insulators and Topological Superconductors* (Princeton University Press, Princeton and Oxford, 2013).

[148] T. Fukui, Y. Hatsugai, and H. Suzuki, J Phys Soc Jpn **74**, 1674 (2005).

[149] E. J. Bergholtz and Z. Liu, arXiv (2013).

[150] S. A. Parameswaran, R. Roy, and S. L. Sondhi, arXiv (2013).

[151] W. Metzner, M. Salmhofer, C. Honerkamp, V. Meden, and K. Schoenhammer, arXiv (2011).

[152] C. Platt, W. Hanke, and R. Thomale, arXiv (2013).

[153] E. Dagotto, Rev Mod Phys **66**, 763 (1994).

[154] G. R. Stewart, Rev Mod Phys **83**, 1589 (2011).

[155] S.-W. Cheong and M. V. Mostovoy, Nat Mater **6**, 13 (2007).

[156] R. Ramesh and N. A. Spaldin, Nat Mater **6**, 21 (2007).

[157] K. F. Wang, J. M. Liu, and Z. F. Ren, Adv Phys **58**, 321 (2009).

[158] H. Y. Hwang, Y. Iwasa, M. Kawasaki, B. Keimer, N. Nagaosa, and Y. Tokura, Nat Mater **11**, 103 (2012).

[159] R. Nandkishore, L. S. Levitov, and A. V. Chubukov, Nat Phys **8**, 158 (2012).

[160] R. Nandkishore, G.-W. Chern, and A. V. Chubukov, Phys Rev Lett **108**, 227204 (2012).

[161] R. Nandkishore and A. V. Chubukov, Phys Rev B **86**, 115426 (2012).

[162] G.-W. Chern, R. M. Fernandes, R. Nandkishore, and A. V. Chubukov, Phys Rev B **86**, 115443 (2012).

[163] G.-W. Chern and C. D. Batista, Phys Rev Lett **109**, 156801 (2012).

[164] M. L. Kiesel, C. Platt, and R. Thomale, Phys Rev Lett **110**, 126405 (2013).

[165] A. V. Maharaj, R. Thomale, and S. Raghu, Phys Rev B **88**, 205121 (2013).

[166] C. Nayak, Phys Rev B **62**, 4880 (2000).

[167] C. Weeks and M. Franz, Phys Rev B **81**, 085105 (2010).

[168] A. G. Grushin, E. V. Castro, A. Cortijo, F. de Juan, M. A. H. Vozmediano, and B. Valenzuela, Phys Rev B **87**, 085136 (2013).

[169] J. Wen, A. Rueegg, C. C. J. Wang, and G. A. Fiete, Phys Rev B **82**, 075125 (2010).

[170] Q. Liu, H. Yao, and T. Ma, Phys Rev B **82**, 045102 (2010).

[171] Y. Zhang, Y. Ran, and A. Vishwanath, Phys Rev B **79**, 245331 (2009).

[172] C. Fang, M. J. Gilbert, and B. A. Bernevig, Phys Rev B **86**, 115112 (2012).

[173] X. Wan, A. M. Turner, A. Vishwanath, and S. Y. Savrasov, Phys Rev B **83**, 205101 (2011).

[174] A. A. Burkov, M. D. Hook, and L. Balents, Phys Rev B **84**, 235126 (2011).

[175] A. A. Burkov and L. Balents, Phys Rev Lett **107**, 127205 (2011).

[176] C. Fang, M. J. Gilbert, X. Dai, and B. A. Bernevig, Phys Rev Lett **108**, 266802 (2012).

[177] F. D. M. Haldane, Phys Rev Lett **93**, 206602 (2004).

[178] J.-M. Hou, Phys Rev Lett **111**, 130403 (2013).

[179] M. A. H. Vozmediano, M. I. Katsnelson, and F. Guinea, Phys Rep **496**, 109 (2010).

[180] S. Gopalakrishnan, P. Ghaemi, and S. Ryu, Phys Rev B **86**, 081403 (2012).

[181] C. Fang, M. J. Gilbert, and B. A. Bernevig, Phys Rev B **88**, 085406 (2013).

[182] K. Sun and E. S. Fradkin, Phys Rev B **78**, 245122 (2008).

[183] T. L. Hughes, E. Prodan, and B. A. Bernevig, Phys Rev B **83**, 245132 (2011).

[184] L. Fu and C. L. Kane, Phys Rev B **76**, 045302 (2007).

[185] E. V. Castro, A. G. Grushin, B. Valenzuela, M. A. H. Vozmediano, A. Cortijo, and F. de Juan, Phys Rev Lett **107**, 106402 (2011).

[186] M. Serbyn and P. A. Lee, Phys Rev B **87**, 174424 (2013).

[187] X.-G. Wen, F. Wilczek, and A. Zee, Phys Rev B **39**, 11413 (1989).

[188] S. Chakravarty, R. Laughlin, D. Morr, and C. Nayak, Phys Rev B **63**, 094503 (2001).

[189] G. Kotliar, Phys Rev B **37**, 3664 (1988).

[190] P. Kotetes and G. Varelogiannis, Epl-Europhys Lett **84**, 37012 (2008).

[191] C.-H. Hsu, S. Raghu, and S. Chakravarty, Phys Rev B **84**, 155111 (2011).

[192] W. Cho, R. Thomale, S. Raghu, and S. A. Kivelson, Phys Rev B **88**, 064505 (2013).

[193] C. Chamon, C.-Y. Hou, R. W. Jackiw, C. Mudry, S.-Y. Pi, and A. Schnyder, Phys Rev Lett **100**, 110405 (2008).

[194] B. Seradjeh, C. Weeks, and M. Franz, Phys Rev B **77**, (2008).

[195] B. Seradjeh and M. Franz, Phys Rev Lett **101**, (2008).

[196] K. S. Novoselov, A. K. Geim, A. V. Morozov, D. Jiang, Y. Zhang, S. V. Dubonos, I. V. Grigorieva, and A. A. Firsov, Science **306**, 666 (2004).

[197] C.-Y. Hou, C. Chamon, and C. Mudry, Phys Rev Lett **98**, (2007).

[198] A. Cortijo, A. G. Grushin, and M. A. H. Vozmediano, Phys Rev B **82**, 195438 (2010).

[199] G. W. Semenoff, Phys Rev Lett **53**, 2449 (1984).

[200] C. W. J. Beenakker, Rev Mod Phys **80**, 1337 (2008).

[201] K. Asano and C. Hotta, Phys Rev B **83**, 245125 (2011).

[202] J. L. Manes, F. Guinea, and M. A. H. Vozmediano, Phys Rev B **75**, (2007).

[203] N. M. R. Peres, Rev Mod Phys **82**, 2673 (2010).

[204] J. L. Manes, Phys Rev B **76**, 045430 (2007).

[205] D. M. Basko, Phys Rev B **78**, 125418 (2008).

[206] V. P. Gusynin, S. G. Sharapov, and J. P. Carbotte, Int J Mod Phys B **21**, 4611 (2007).

[207] H. M. Guo and M. Franz, Phys Rev B **80**, 113102 (2009).

[208] L. Messio, C. Lhuillier, and G. Misguich, Phys Rev B **83**, 184401 (2011).

[209] G.-W. Chern, A. Rahmani, I. Martin, and C. D. Batista, arXiv (2012).

[210] H. Ishizuka and Y. Motome, Phys Rev B **87**, 081105 (2013).

[211] M. Daghofer and M. Hohenadler, arXiv (2013).